NASA TECHNICAL NOTE

NASA TN D-2350

NASA TN D-2350

AFTERBODY PRESSURES ON TWO-DIMENSIONAL BOATTAILED BODIES HAVING TURBULENT BOUNDARY LAYERS AT MACH 5.98

by W. Frank Staylor and Theodore J. Goldberg

Langley Research Center
Langley Station, Hampton, Va.

NATIONAL AERONAUTICS AND SPACE ADMINISTRATION • WASHINGTON, D. C. • JULY 1964

AFTERBODY PRESSURES ON TWO-DIMENSIONAL BOATTAILED BODIES HAVING TURBULENT BOUNDARY LAYERS AT MACH 5.98

By W. Frank Staylor and Theodore J. Goldberg

Langley Research Center
Langley Station, Hampton, Va.

NATIONAL AERONAUTICS AND SPACE ADMINISTRATION

For sale by the Office of Technical Services, Department of Commerce,
Washington, D.C. 20230 -- Price $1.00

AFTERBODY PRESSURES ON TWO-DIMENSIONAL BOATTAILED BODIES HAVING TURBULENT BOUNDARY LAYERS AT MACH 5.98

By W. Frank Staylor and Theodore J. Goldberg
Langley Research Center

SUMMARY

An investigation has been conducted on a series of two-dimensional afterbodies to determine the effects of boattailing and angle of attack upon base and boattail pressures. Afterbodies with boattail angles from 0° to 18° at angles of attack up to 14° were investigated at a free-stream Reynolds number sufficient to cause fully turbulent boundary layers to exist ahead of the afterbodies. The models were tested at a free-stream Mach number of 5.98 which resulted in surface Mach numbers from approximately 3 to 7.

A simple semiempirical method is presented for estimating base pressures for boattailed bodies at angle of attack which is the result of a correlation of base-pressure data from previous studies and the present investigation. This method is a modification and extension of previous work and gives a good estimate for existing base-pressure data between the Mach numbers of 1.4 to 6.0. The empirical estimation of boattail pressures made possible predictions of afterbody drag. At zero angle of attack a near minimum afterbody drag was obtained between the Mach numbers of 2 to 6 both experimentally and by calculation with boattail angles ranging from 6° to 12°.

INTRODUCTION

Theoretical and experimental investigations have shown that afterbody drag constitutes a substantial portion of the total drag on two-dimensional airfoils at supersonic speeds (for example, see refs. 1 to 11). Chapman (refs. 1, 2, and 7) reports that in certain cases afterbody drag can amount to as much as three-fourths of the total airfoil drag. At high-supersonic and hypersonic speeds, theoretical and limited experimental investigations have indicated that afterbody drag is still a major design parameter for optimum lift-drag profiles although its influence is somewhat lessened.

Many of the existing two-dimensional afterbody investigations include the effects of angle of attack and boattailing upon base pressure; however, in most of these studies the pressures on the boattail surfaces were not measured. Therefore, experimental data for the determination of total afterbody-pressure drag are limited at supersonic Mach numbers and completely lacking in the hypersonic range. The verification of existing supersonic methods for

predicting base pressure at hypersonic Mach numbers has not been possible because of the lack of such data.

The purpose of the present investigation was to obtain hypersonic base- and boattail-pressure data at angles of attack for two-dimensional bodies having turbulent boundary layers. This investigation was limited to turbulent boundary layers because previous investigations have shown that Reynolds number had a negligible effect on base pressure for bodies having fully turbulent boundary layers (refs. 1, 2, and 9) which would be representative of most full-scale hypersonic applications. This investigation was performed in the Langley 20-inch Mach 6 tunnel at a free-stream Reynolds number of 7.7×10^6 per foot.

SYMBOLS

C_A component of axial-force coefficient due to afterbody drag

$C_{p,\infty}$ pressure coefficient based on free-stream conditions, $\frac{p - p_\infty}{q_\infty}$

$C_{p,0}$ pressure coefficient based on conditions ahead of the base, $\frac{p - p_0}{q_0}$

l boattail length

M Mach number

p static pressure

q dynamic pressure

R surface Reynolds number at junction of model and afterbody

s surface distance measured from center of base

t model thickness

α angle of attack

β boattail angle

γ equivalent Prandtl-Meyer expansion angle from boattail to base, $\nu_1 - \nu_0$

δ critical turning angle (see eqs. (2) to (4))

ϵ equivalent Prandtl-Meyer expansion angle from model to boattail, $\nu_0 - \nu_m$

ν Prandtl-Meyer expansion angle

Subscripts:

∞ free-stream conditions

0 conditions ahead of base

1 conditions ahead of trailing shock

b conditions at base

m conditions on model surface ahead of boattail

min minimum

Superscript:

' average conditions on base or boattail surfaces

APPARATUS AND TEST METHODS

Wind Tunnel

The present investigation was conducted in the Langley 20-inch Mach 6 tunnel. This tunnel is an intermittent tunnel that exhausts through a movable second minimum to atmosphere with the aid of an annular ejector. Stagnation pressure and temperature were approximately 400 psia and 400° F corresponding to a Reynolds number per foot of 7.7×10^6 for all tests. A more complete description of the tunnel is given in reference 12.

Model and Support

Presented in figure 1 are sketches and photographs of the model, support, and afterbodies. The model was 13 inches long, 9 inches wide, and 1 inch thick with a 15° half-angle wedge nose with a maximum leading-edge diameter of 0.005 inch. Afterbody configurations having boattail angles from 0° to 18°, in 3° increments, plus one circular-arc configuration were attached to the rear of the model each with 13 pressure orifices located at the midspan. Two additional orifices were located on the model at the midspan, one on the upper and lower surface. Transition strips were bonded to the upper and lower surfaces for all but one of the test runs. These strips consisted of 0.050-inch-diameter grit and were 0.3 and 0.6 inch wide on the wedge and plate surfaces, respectively, as shown in figure 1(b).

The model was supported from its sides in the center of the test section by four vertical struts and was pivoted about the rear struts for angle-of-attack variation (see fig. 1(c)). The model was tested at nominal angles of

attack of 0°, $\pm 3^\circ$, $\pm 6^\circ$, $\pm 9^\circ$, and $\pm 12^\circ$, but the actual measured angles varied as much as 2° from these values as a result of wind loads on the model and support. At both positive and negative angles of attack the pressures were equal on the windward surfaces; however, small pressure differences were noted on the leeward surfaces at high angles of attack. Therefore, only positive angle-of-attack data (leeward surface opposite to the support system) are presented.

A flat-plate model with similar dimensions was previously tested in the Langley 20-inch Mach 6 tunnel at angles of attack from -8° to 5° (ref. 12). This model had several orifices located along the span 2.5 inches from each edge, and it was found that the pressures were constant in the spanwise direction.

Test Methods and Techniques

Static pressures on the model and afterbodies were recorded by photographing two multiple-tube manometers - one with butyl phthalate as the fluid for measuring pressures less than 1.0 psia, the other with mercury for higher pressures. Tunnel stagnation pressure was measured with a Bourdon gage which was photographed simultaneously with the manometers. All calculations were based on a nominal free-stream Mach number of 5.98. The estimated maximum inaccuracies of the pressure coefficients are:

$\Delta C_{p,\infty}$ due to Mach number variation	± 0.0020
$\Delta C_{p,\infty}$ due to pressure measurement errors	± 0.0015 for $C_{p,\infty} < 0.12$
$\Delta C_{p,\infty}$ due to pressure measurement errors	± 0.0090 for $C_{p,\infty} > 0.12$

The angles of attack were set at nominal angles of 0°, 3°, 6°, 9°, and 12°, but the actual angles as determined from photographs are believed accurate to $\pm 0.1^\circ$.

RESULTS AND DISCUSSION

Data Presentation

Variation of Mach number and Reynolds number.- Presented in figure 2 is a plot of Mach number on the windward and leeward surfaces of the model as a function of angle of attack. Shock-expansion and experimental values ($\beta = 0^\circ$ and 12°) based on the ratio of measured static pressure to theoretical total pressure behind the oblique shock are shown. A comparison of the experimental Mach numbers obtained with the 0° and 12° boattails indicates that the afterbodies do not influence flow conditions on the model. These values agree with the trend of the shock-expansion method at all angles of attack on the windward surface and to about 5° angle of attack on the leeward surface beyond which angle flow separation is believed to occur. Mach numbers obtained by the shock-expansion method are used for all subsequent calculations.

The surface Reynolds number at the junction of the model and afterbody is plotted against Mach number on the model surface in figure 3. The Reynolds numbers were calculated with the assumption that shock-expansion flow existed on the model surfaces. Data from a previous two-dimensional boundary-layer investigation conducted in the same tunnel are included in figure 3 in order to establish regions of boundary-layer transition (ref. 13). It should be noted that these data from reference 13 were for natural transition (no roughness) on flat plates and therefore had a turbulence level less than that of the present investigation. Therefore, the boundary layer at the junction is believed to be fully turbulent on the windward surface and also on the leeward surface to the point of flow separation ($\alpha < 5^\circ$).

Pressure distributions.- Presented in figure 4 are the pressure distributions on the boattailed afterbodies at angles of attack. The pressures generally decreased slightly on the windward boattail toward the base but were essentially constant on the base and leeward boattail for each wedge afterbody at a given angle of attack. Large pressure gradients existed along the windward surface of the circular-arc boattail (fig. 4(h)) which were due to the continuous expansion of the flow along the curved surface. These data are included in some of the following figures, but will not be discussed further. The removal of the roughness strips (fig. 4(e)) had little, if any, effect on the afterbody pressures when the small differences in angles of attack of the model and the accuracy of the data are considered; this further substantiates the existence of a fully turbulent boundary layer.

Schlieren photographs.- Presented in figure 5 are typical schlieren photographs of the flow phenomena in the region of the base for the 0°, 6°, and 12° afterbodies at various angles of attack. These photographs are included only to serve as visual aids since no attempt was made to measure flow angles and compare them with theoretical or other experimental values. The general quality of the photographs is poor; however, the boundaries of the base wake and the trailing shock waves may be seen in most cases. The boundary layers on the leeward surface are identified as the dark regions above the afterbodies and appear to separate from the surface at the higher angles of attack. The dark spots in the lower right-hand corner of the photographs were caused by chips in the tunnel windows.

Prediction of Afterbody Pressures

Windward boattail.- The experimental pressures were not constant along the windward surface of the wedge boattails but are treated as an integrated average pressure in further discussions since the variations were usually small. In figure 6 the experimental average pressures for these surfaces are presented and compared with those calculated by the shock-expansion method. Both the experimental and calculated pressures increase with angle of attack and decrease with boattail angle, as one might expect; however, the shock-expansion method generally underpredicts the experimental pressures. This underprediction is apparently caused by the failure of the flow to expand through the full boattail angle β. Boundary-layer growth and/or separation are believed to be the cause of this apparent underexpansion of the flow.

The equivalent Prandtl-Meyer expansion angles ϵ necessary to calculate the experimental average pressures on the boattails are given in figure 7 as a function of β and M_m. Also, data are included from a similar boattailed afterbody investigation conducted at a supersonic Mach number ($M_m = 2.30$) at zero angle of attack (ref. 5). It is seen that for a given boattail angle the equivalent turning angles are generally less than β and decrease with increased surface Mach number M_m. In the absence of such data, one would normally assume that the flow had expanded through the full angle β which could result in large pressure and Mach number errors on the boattail surfaces. Therefore a simple empirical equation,

$$\epsilon = (1.39 - 0.19M_m)\beta \tag{1}$$

is presented which, with reasonable accuracy, can be used to estimate the turning angles obtained experimentally. Equation (1) was used to calculate the pressures on the 0°, 6°, 12°, and 18° windward boattail surfaces, and the results are shown in figure 8. The estimates show good agreement with the data and are a definite improvement over the shock-expansion method ($\epsilon = \beta$) shown in figure 6.

Base.- Numerous two-dimensional base-pressure investigations conducted at low-supersonic speeds have supplied data from which various theoretical- and empirical-prediction methods were conceived. Essentially, most of these methods are concerned with predicting the flow-expansion angle at the model base from which base pressure can be calculated. A method proposed by Love (ref. 3) utilizes the analogy between forward- and rearward-facing steps to determine a critical turning angle δ which is equal to the expansion angle γ at the base of a nonboattailed body ($\beta = 0^\circ$) at zero angle of attack. This proposal is represented by the equation

$$\delta = \gamma \tag{2}$$

and can be visualized by an inspection of sketch 1. Cortright and Schroeder (ref. 6) have further proposed that the critical turning angle may be used to estimate base pressures on boattailed bodies at zero angle of attack with the

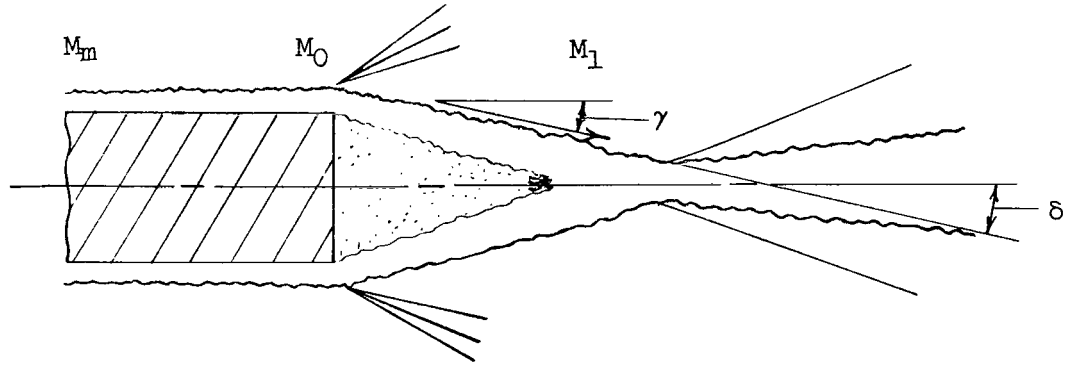

Sketch 1

assumption that δ is a function only of the Mach number ahead of the base. Their original proposal is given by the equation

$$\delta = \gamma + \beta \tag{3a}$$

but in the following discussions β is replaced by ϵ (see sketch 2) giving the following equation:

$$\delta = \gamma + \epsilon \tag{3b}$$

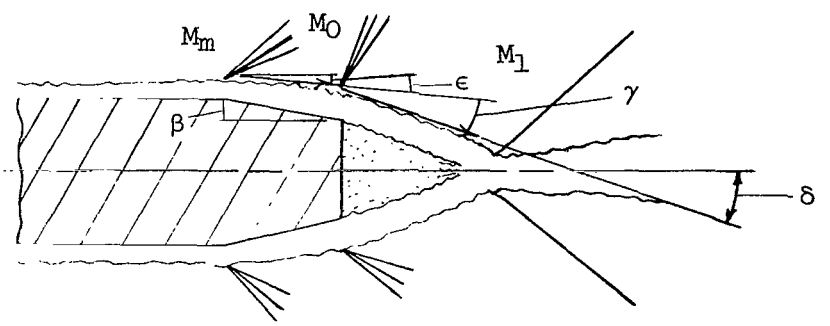

Sketch 2

Presented in figure 9 are the critical turning angles calculated both from experimental base-pressure data ($\alpha = 0^\circ$; $\beta \geqq 0^\circ$) with the use of equations (1) to (3) and from forward-facing-step data (see ref. 3). The base-pressure coefficients shown in figure 10 were determined by expanding the flow at a Mach number of M_0 through the appropriate angle δ obtained from figure 9. The plain and flagged symbols in these figures denote pressure data ($\alpha = 0^\circ$) for $\beta = 0^\circ$ and $\beta > 0^\circ$, respectively. In the present study it is proposed that the critical turning angle may further be used to estimate base pressures on boattailed bodies at small angles of attack (see sketch 3) with the use of the equation

$$\delta = \gamma + \epsilon - \alpha \tag{4}$$

It is assumed that the base pressure is primarily a function of the flow conditions on the windward surfaces and that both δ and ϵ are determined from

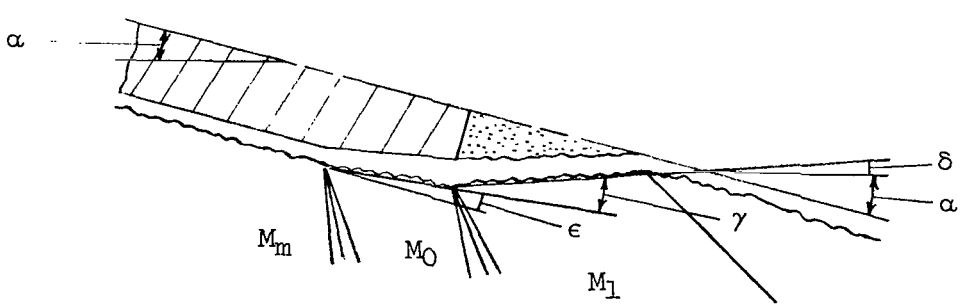

Sketch 3

these conditions. Critical turning angles were calculated with equation (4) from pressure data at angles of attacks up to 14° and then were converted to $C_{p,0}$ values. These data are denoted as solid symbols in figure 10, and the validity of the present proposal may be seen.

Equation (4) reduces to equations (2) and (3b) when the appropriate terms are dropped to satisfy the requirements originally proposed by Love ($\alpha = \beta = 0°$) and Cortright and Schroeder ($\alpha = 0°$). Therefore, equations (1) and (4) together with figure 9 can be used to estimate the base pressures on boattailed bodies at angles of attack from Mach numbers of 1.4 to 6.0. An example calculation is presented in the appendix to clarify details that are not discussed here.

In figure 11(a) experimental base values $C'_{p,\infty}$ are presented and compared with the calculated values for boattail angles of 0°, 6°, 12°, and 18°. The agreement is very good for afterbodies with small boattail angles throughout the angle-of-attack range of the investigation. The present method overpredicts base pressures on the $\beta = 15°$ and $\beta = 18°$ afterbodies which can be attributed to total separation of the flow from the boattail surfaces. The pressures were essentially equal on all surfaces of these afterbodies at small angles of attack (figs. 4(f) and 4(g)) which indicates that the flow had separated at the junctions of the model and afterbodies. In effect, the flow does not sense the existence of these afterbodies and their base pressures, in general, can be better predicted by the $\beta = 0°$ base-pressure estimate (see sketch 4).

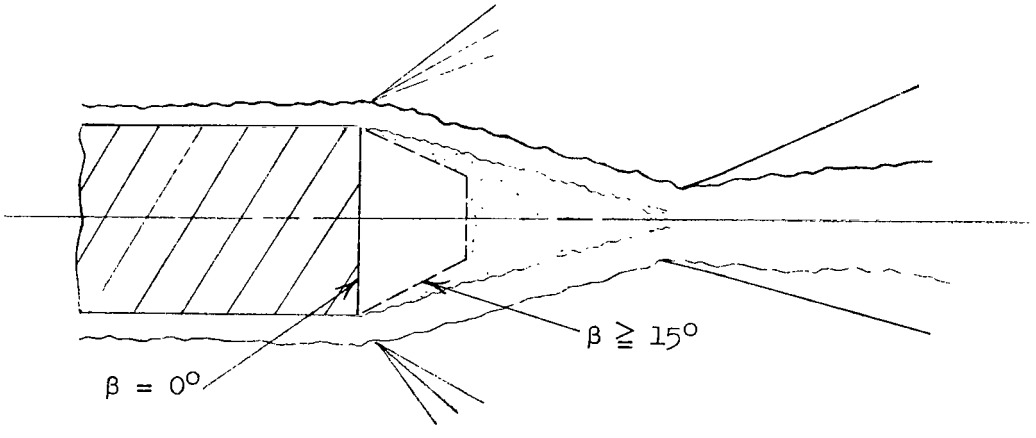

Sketch 4

Leeward boattail.- Experimental leeward boattail $C'_{p,\infty}$ values are presented in figure 11(b) along with estimated values which are complicated by flow separation occurring forward of the afterbody at $\alpha > 5°$. Equation (1) may be used to estimate the pressures on the leeward boattail surfaces in a manner similar to that employed for the windward surfaces when the flow is believed to be attached. Experimental data show that the leeward boattail pressure is approximately equal to the base pressure at high angles of attack;

these pressures are approximated by the base-pressure values when the flow is believed to be separated forward of the afterbody.

Afterbody Drag

Experimental and estimated components of axial-force coefficient due to afterbody drag obtained from integration of the experimental and estimated pressures over the afterbody surfaces are presented in figure 12. At zero angle of attack, afterbody drag was reduced from 0.0256 for $\beta = 0^\circ$ to about 0.0195 (25-percent reduction) for $\beta = 6^\circ$, 9°, or 12°. Drag on the boattailed afterbodies decreased with increasing angle of attack with minimum drag occurring on the 12° afterbody. At $\alpha = 13^\circ$ afterbody drag was reduced as much as 70 percent as the result of boattailing the model. The experimental drag coefficients are well predicted by the present estimates for $\beta \leq 12^\circ$ but are underpredicted for larger angles because of flow separation. As previously mentioned, a better estimate may be obtained for the larger boattail angles by assuming that the $\beta = 0^\circ$ base-pressure estimates exist on the base and leeward boattail surfaces.

Experimental and calculated minimum afterbody-drag coefficients and their associated boattail angles at zero angle of attack are presented in figure 13. These coefficients are based on afterbody length-to-height ratio of 1.15 which approximates the models used for the present investigation and for those of reference 5. Experimentally, the minimum drag coefficients were found to be relatively insensitive to boattail angle within $\pm 3^\circ$; minimum drag occurred both experimentally and theoretically at approximately $\beta = 9^\circ$ between the Mach numbers of 2 to 6.

CONCLUDING REMARKS

Afterbody pressures have been investigated at a free-stream Mach number of 5.98 along a series of two-dimensional boattailed bodies at various angles of attack. A simple semiempirical method for estimating base pressures for boattailed bodies at angle of attack with turbulent boundary layers is presented which is a modification and extension of previous methods. The present method is the result of a correlation of base-pressure data from previous studies and the present investigations and gives a good estimate for these data between the local Mach numbers of 1.4 to 6.0. Pressures on the boattails could not be predicted by the Prandtl-Meyer method by assuming that the flow ahead had turned the full boattail angle; therefore, an empirical equation is presented which relates the equivalent turning angle as a function of boattail angle and Mach number just ahead of the boattail.

It was found that base drag can be substantially reduced with the use of short length, boattailed afterbodies. At zero angle of attack a near minimum drag was obtained between the local Mach numbers of 2 to 6 both experimentally

and by calculation with boattail angles ranging from 6° to 12°. At angles of attack, minimum drag was obtained experimentally with 12° boattail for the present investigation.

Langley Research Center,
National Aeronautics and Space Administration,
Langley Station, Hampton, Va., February 29, 1964.

APPENDIX

EXAMPLE CALCULATION

Presented here is an example of the calculation procedure for obtaining boattail and base-pressure coefficients by the method presented in the body of the report. Example calculations are made for the two-dimensional boattailed body shown in sketch 5 for a free-stream Mach number of 5.0. Both the angle of attack and boattail angle are 5° and the short boattail length ($l/t = 1.15$)

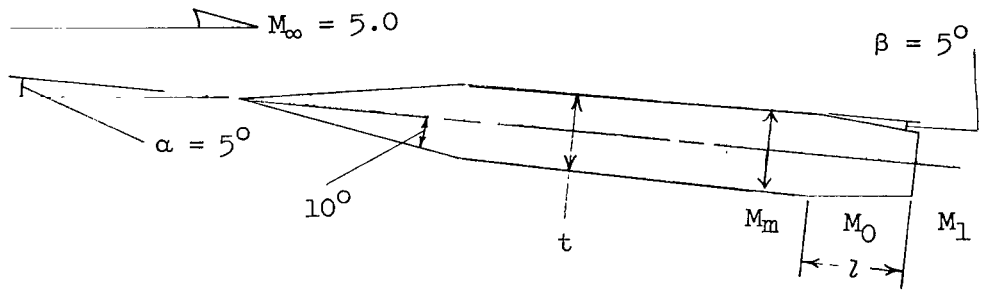

Sketch 5

is consistent with the present analysis. It is assumed that the boundary layers are fully turbulent on both the windward and leeward surfaces ahead of the boattails and that the shock-expansion method can be used to calculate the flow properties on these surfaces. These properties are:

Windward:

$$M_m = 4.22 \qquad \nu_m = 68.58^\circ \qquad p_m/p_\infty = 1.80$$

Leeward:

$$M_m = 5.55 \qquad \nu_m = 81.64^\circ \qquad p_m/p_\infty = 0.52$$

With the use of equation (1) ($\epsilon = (1.39 - 0.19M_m)\beta$), the equivalent Prandtl-Meyer expansion angles can be calculated which will allow the computation of the other flow properties on the boattails:

Windward:

$$\epsilon = \left[1.39 - 0.19(4.22)\right] \times 5^\circ = 2.95^\circ \qquad \nu_0 = 68.58^\circ + 2.95^\circ = 71.53^\circ$$

$$M_0 = 4.47 \qquad p_0/p_\infty = 1.31 \qquad C_{p,\infty} = 0.0176$$

Leeward:

$$\epsilon = \left[1.39 - 0.19(5.55)\right] \times 5^\circ = 1.68^\circ \qquad \nu_0 = 81.64^\circ + 1.68^\circ = 83.32^\circ$$

$$M_0 = 5.77 \qquad p_0/p_\infty = 0.41 \qquad C_{p,\infty} = -0.0336$$

As stated previously in the text, the base pressures were found to be primarily a function of the flow properties on the windward boattails; therefore, a critical turning angle δ of 9.35° is obtained from figure 9 for the windward boattail Mach number of 4.47. The base-pressure coefficients can now be evaluated by calculating γ (see sketch 3) in equation (4).

$$\gamma = \delta + \alpha - \epsilon = 9.35^\circ + 5.00^\circ - 2.95^\circ = 11.40^\circ$$

$$\nu_1 = 71.53^\circ + 11.40^\circ = 82.93^\circ$$

$$M_1 = 5.72 \qquad p_b/p_\infty = 0.31 \qquad C_{p,\infty} = -0.0394$$

The axial component of afterbody-drag coefficient for a unit span is,

$$C_A = -\left[(l/t)\tan\beta(C_{p,\infty})_{\text{Windward boattail}} + (l/t)\tan\beta(C_{p,\infty})_{\text{Leeward boattail}} + \left(1 - 2(l/t)\tan\beta\right)(C_{p,\infty})_{\text{Base}}\right]$$

$$= -\left[(0.1)(0.0176) + (0.1)(-0.0336) + (0.8)(-0.0394)\right] = 0.0331$$

assuming that the flow is attached to the leeward surface ahead of the boattail. If it were assumed that the flow is separated from this surface, the leeward boattail pressure coefficient, -0.0336, should be replaced by the base-pressure coefficient, -0.0394. The resulting afterbody-drag coefficient would therefore be slightly increased to 0.0337.

REFERENCES

1. Chapman, Dean R.: An Analysis of Base Pressure at Supersonic Velocities and Comparison With Experiment. NACA Rep. 1051, 1951. (Supersedes NACA TN 2137.)

2. Chapman, Dean R., Wimbrow, William R., and Kester, Robert H.: Experimental Investigation of Base Pressure on Blunt-Trailing-Edge Wings at Supersonic Velocities. NACA Rep. 1109, 1952. (Supersedes NACA TN 2611.)

3. Love, Eugene S.: Base Pressure at Supersonic Speeds on Two-Dimensional Airfoils and on Bodies of Revolution With and Without Fins Having Turbulent Boundary Layers. NACA TN 3819, 1957. (Supersedes NACA RM L53C02.)

4. Goin, Kennith L.: Effects of Plan Form, Airfoil Section, and Angle of Attack on the Pressures Along the Base of Blunt-Trailing-Edge Wings at Mach Numbers of 1.41, 1.62, and 1.96. NACA RM L52D21, 1952.

5. Fuller, L., and Reid, J.: Experiments on Two-Dimensional Base Flow at M = 2.4. R. & M. No. 3064, British A.R.C., 1958.

6. Cortright, Edgar M., Jr., and Schroeder, Albert H.: Investigation at Mach Number 1.91 of Side and Base Pressure Distributions Over Conical Boattails Without and With Jet Flow Issuing From Base. NACA RM E51F26, 1951.

7. Chapman, Dean R.: Airfoil Profiles for Minimum Pressure Drag at Supersonic Velocities - Application of Shock-Expansion Theory, Including Consideration of Hypersonic Range. NACA TN 2787, 1952.

8. Syvertson, Clarence A., and Gloria, Hermilo R.: An Experimental Investigation of the Zero-Lift-Drag Characteristics of Symmetrical Blunt-Trailing-Edge Airfoils at Mach Numbers From 2.7 to 5.0. NACA RM A53B02, 1953.

9. Reller, John O., Jr., and Hamaker, Frank M.: An Experimental Investigation of the Base Pressure Characteristics of Nonlifting Bodies of Revolution at Mach Numbers From 2.73 to 4.98. NACA TN 3393, 1955. (Supersedes NACA RM A52E20.)

10. Chapman, Dean R.: Reduction of Profile Drag at Supersonic Velocities by the Use of Airfoil Sections Having a Blunt Trailing Edge. NACA TN 3503, 1955. (Supersedes NACA RM A9H11.)

11. Katzen, Elliott D., Kuehn, Donald M., and Hill, William A., Jr.: Investigation of the Effects of Profile Shape on the Aerodynamic and Structural Characteristics of Thin, Two-Dimensional Airfoils at Supersonic Speeds. NACA TN 4039, 1957. (Supersedes NACA RM A54B08a.)

12. Sterrett, James R., and Emery, James C.: Extension of Boundary-Layer-Separation Criteria to a Mach Number of 6.5 by Utilizing Flat Plates With Forward-Facing Steps. NASA TN D-618, 1960.

13. Holloway, Paul F., and Sterrett, James R.: Effect of Controlled Surface Roughness on Boundary-Layer Transition and Heat Transfer at Mach Numbers of 4.8 and 6.0. NASA TN D-2054, 1964.

14. Strack, S. L.: Heat Transfer at Reattachment of a Turbulent Boundary Layer. Doc. No. D2-22430, The Boeing Company, Apr. 30, 1963.

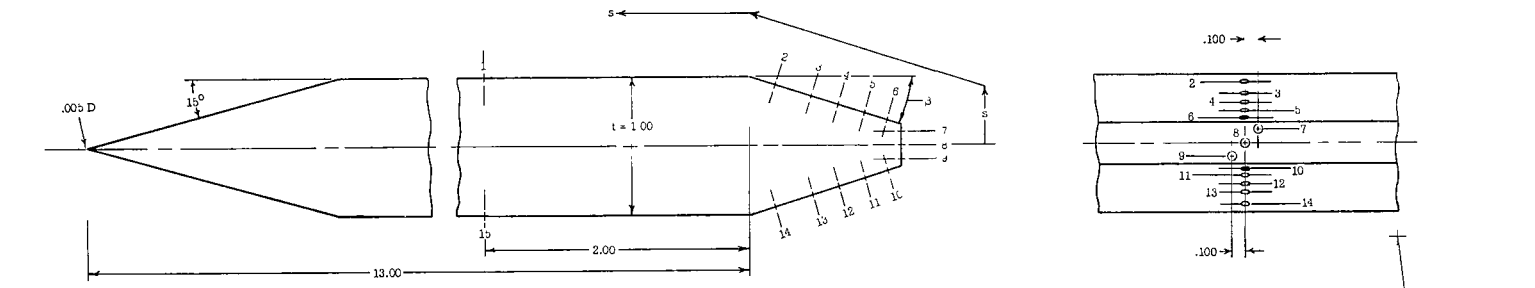

0° boattail	
Orifice	s/t
1	3.650
2	1.500
3	1.250
4	1.000
5	.840
6	.700
7	.125
8	.000
9	-.125
10	-.700
11	-.840
12	-1.000
13	-1.250
14	-1.500
15	-3.650

3° boattail	
Orifice	s/t
1	3.600
2	1.440
3	1.190
4	.940
5	.780
6	.640
7	.125
8	.000
9	-.125
10	-.640
11	-.780
12	-.940
13	-1.190
14	-1.440
15	-3.600

6° boattail	
Orifice	s/t
1	3.550
2	1.390
3	1.140
4	.890
5	.730
6	.590
7	.125
8	.000
9	-.125
10	-.590
11	-.730
12	-.890
13	-1.140
14	-1.390
15	-3.550

9° boattail	
Orifice	s/t
1	3.480
2	1.320
3	1.140
4	.890
5	.730
6	.590
7	.125
8	.000
9	-.125
10	-.590
11	-.730
12	-.890
13	-1.140
14	-1.320
15	-3.480

12° boattail	
Orifice	s/t
1	3.450
2	1.290
3	1.030
4	.780
5	.610
6	.470
7	.130
8	.000
9	-.130
10	-.470
11	-.610
12	-.780
13	-1.030
14	-1.290
15	-3.450

15° boattail	
Orifice	s/t
1	3.175
2	1.195
3	.945
4	.695
5	.545
6	.365
7	.100
8	.000
9	-.100
10	-.365
11	-.545
12	-.695
13	-.945
14	-1.195
15	-3.175

16° boattail	
Orifice	s/t
1	3.100
2	1.000
3	.870
4	.650
5	.520
6	.360
7	.080
8	.000
9	-.080
10	-.340
11	-.520
12	-.650
13	-.870
14	-1.090
15	-3.100

Circular-arc boattail		
Orifice	s/t	ρ, deg
1	3.[illegible]	[illegible]
2	1.[illegible]	[illegible]
3	1.[illegible]	[illegible]
4	.[illegible]	[illegible]
5	.[illegible]	[illegible]
6	.[illegible]	[illegible]
7	.[illegible]	[illegible]
8	.000	90.0
9	-.[illegible]	[illegible]
10	-.[illegible]	[illegible]
11	-.[illegible]	[illegible]
12	-.[illegible]	[illegible]
13	-1.[illegible]	[illegible]
14	-1.[illegible]	[illegible]
15	-3.190	0.0

(a) Sketches of model and afterbodies.

Figure 1.- Sketch and photographs of model, support, and afterbodies.

(b) Model and afterbodies. L-60-1680

Figure 1.- Continued.

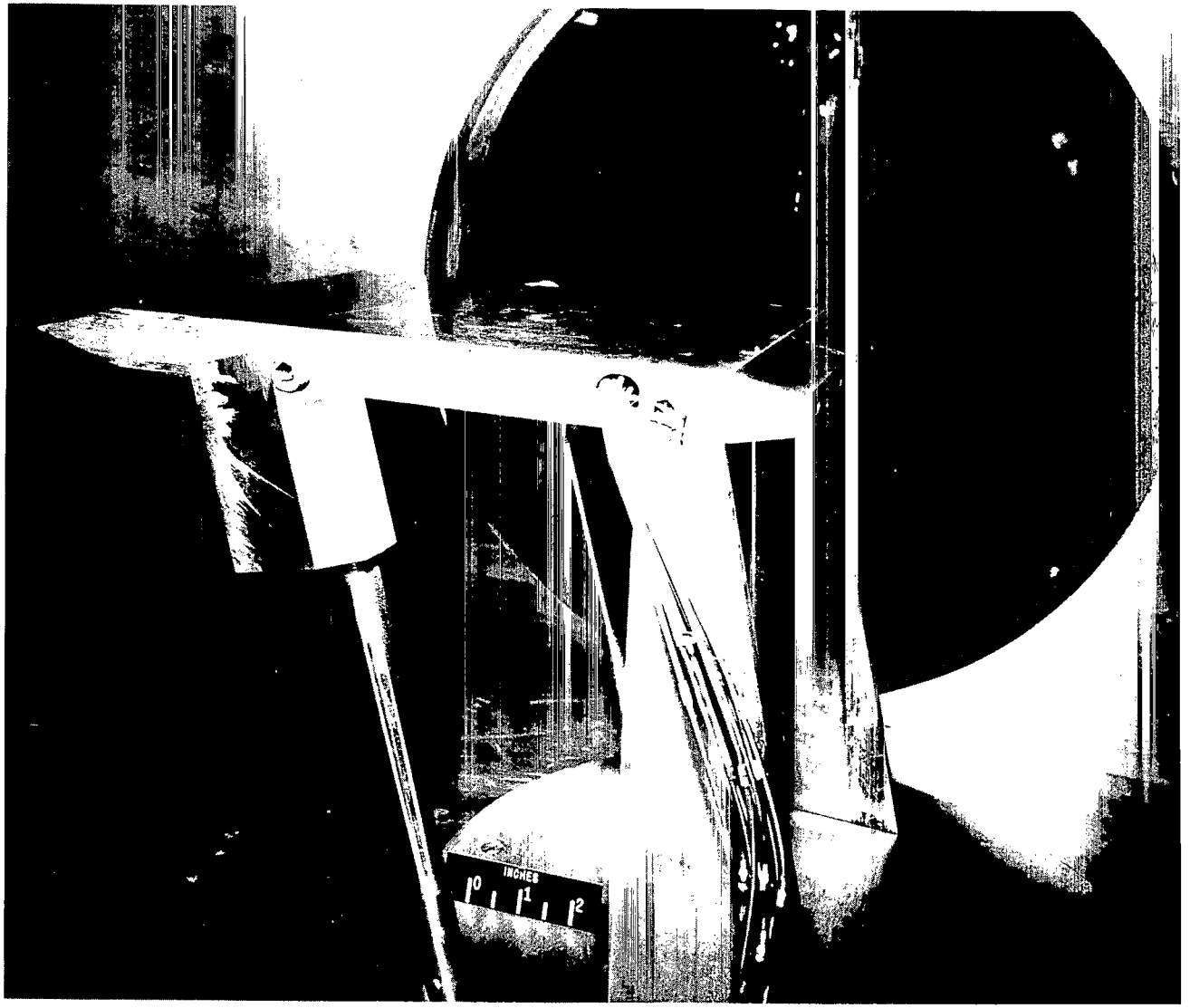

(c) Model-support assembly. L-60-1672

Figure 1.- Concluded.

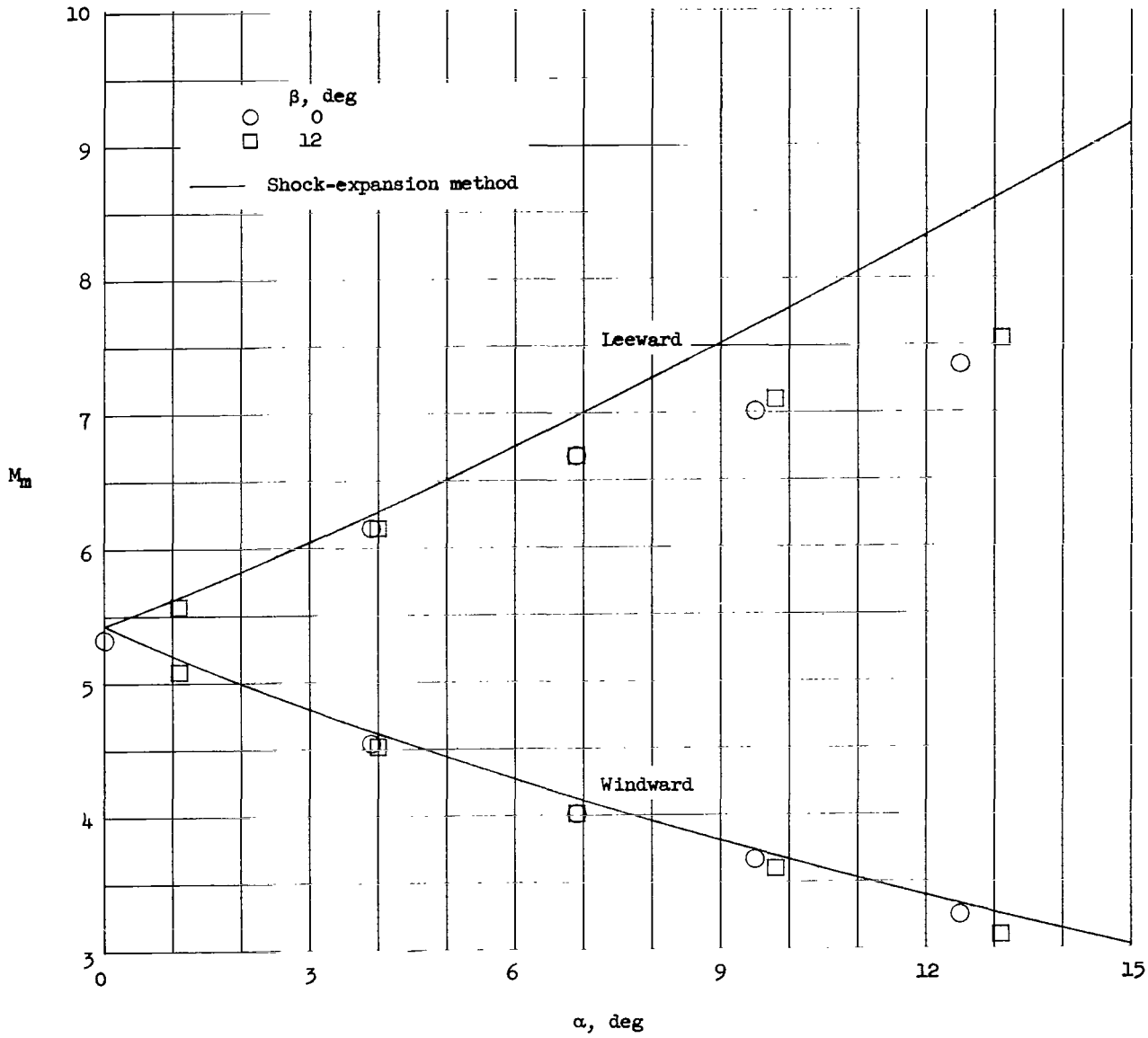

Figure 2.- Variation of Mach number on windward and leeward model surfaces with angle of attack.

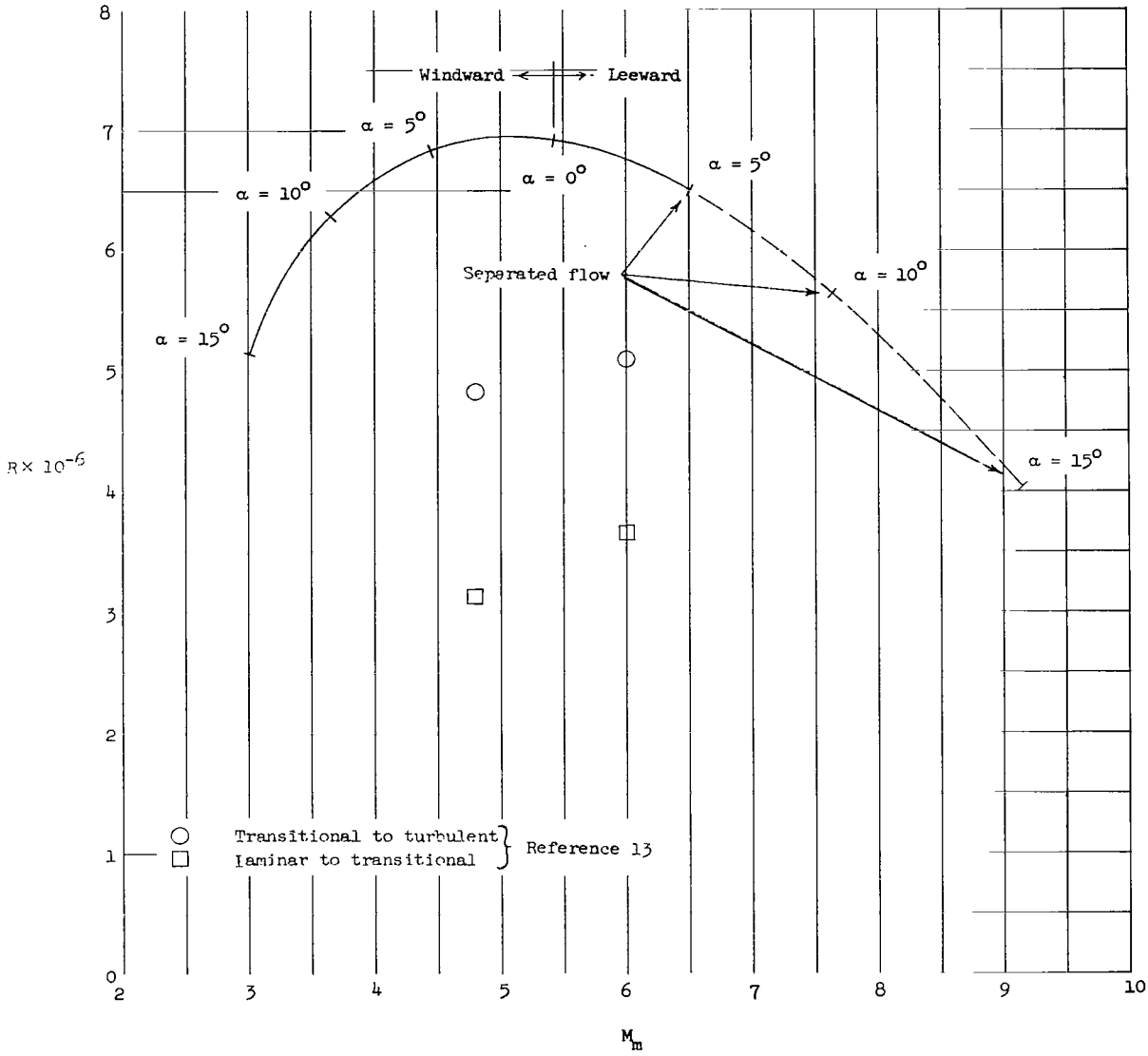

Figure 3.- Variation of surface Reynolds number at junction of model and afterbodies with surface Mach number.

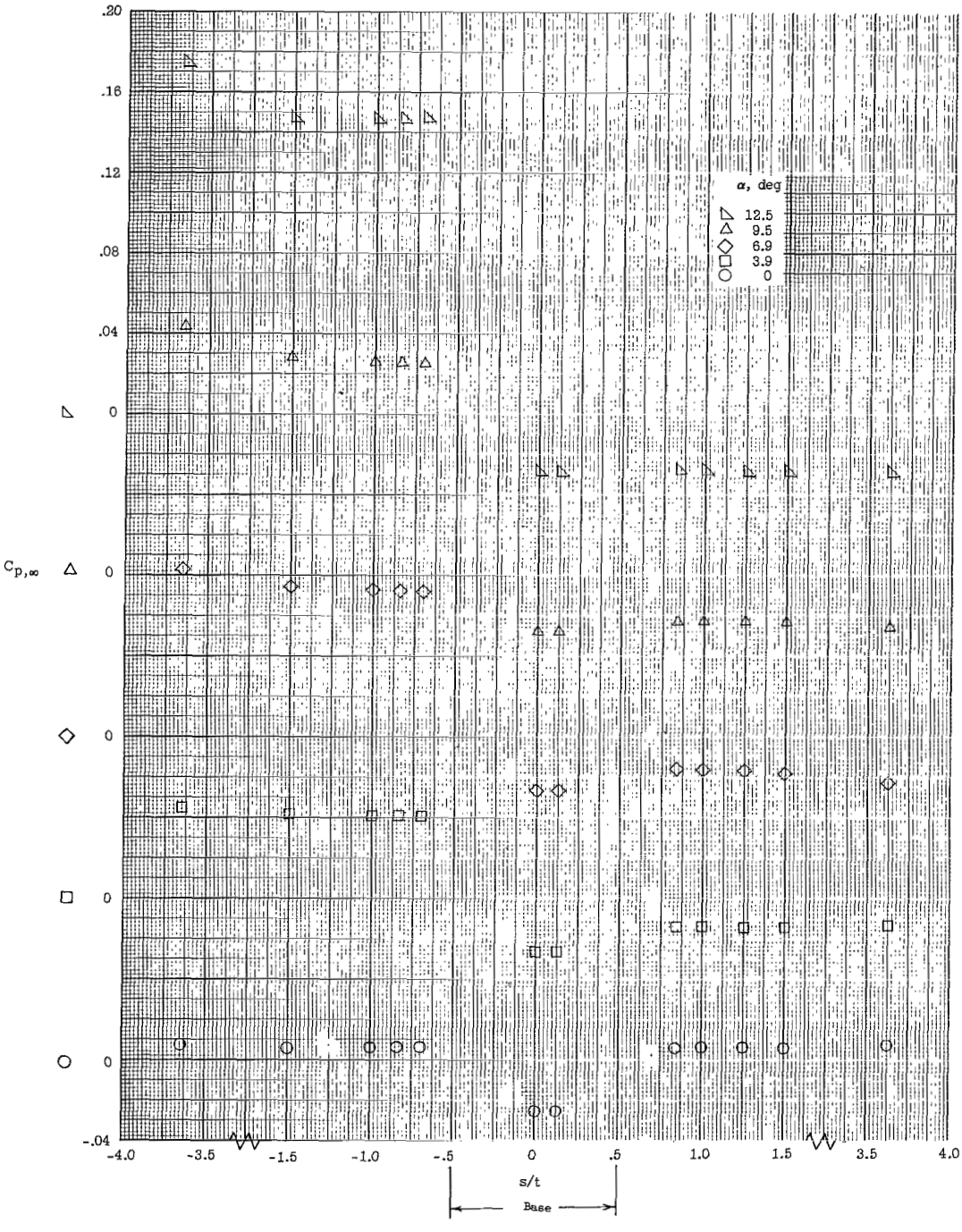

(a) $\beta = 0^{o}$.

Figure 4.- Afterbody pressure distributions at various angles of attack for a series of boattailed afterbodies.

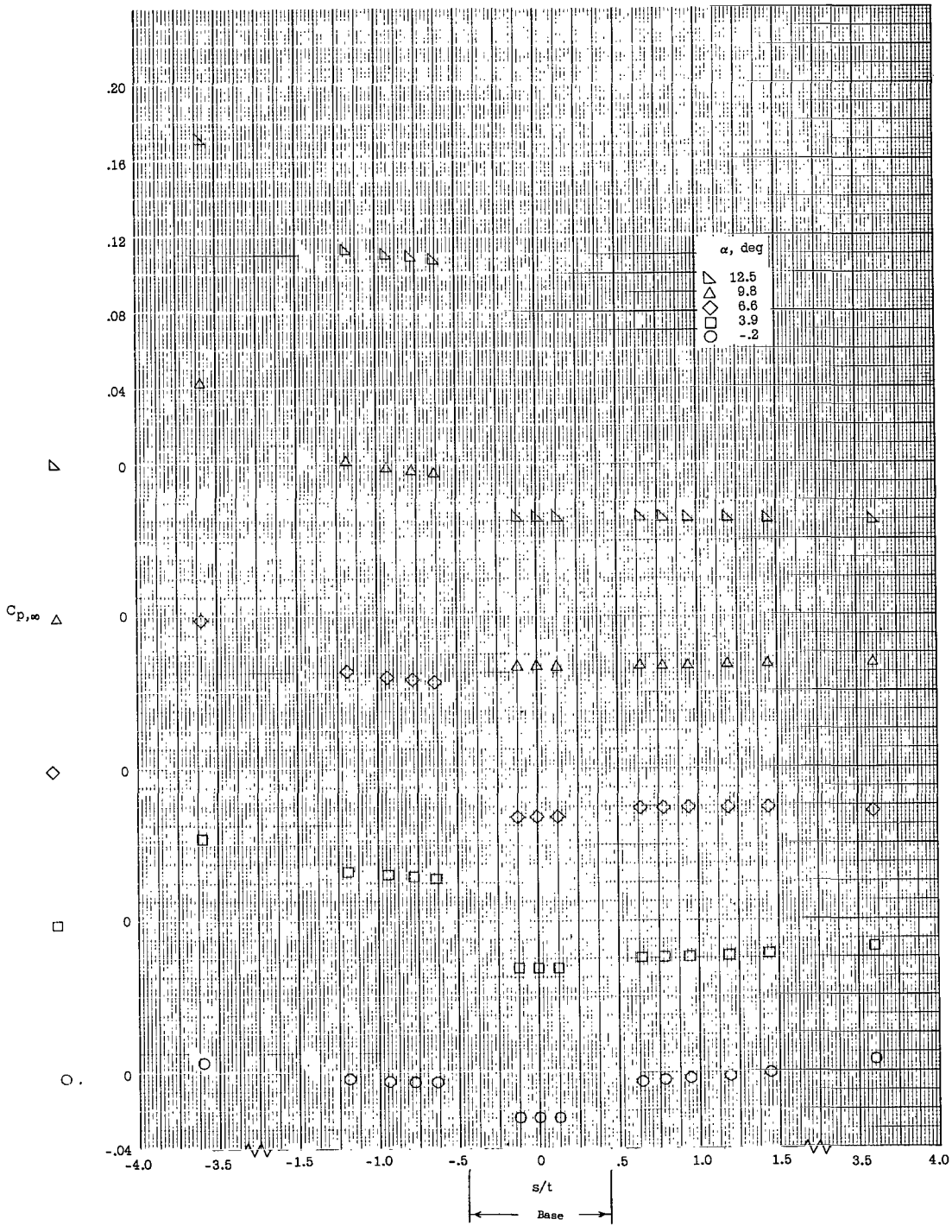

(b) $\beta = 3^{\circ}$.

Figure 4.- Continued.

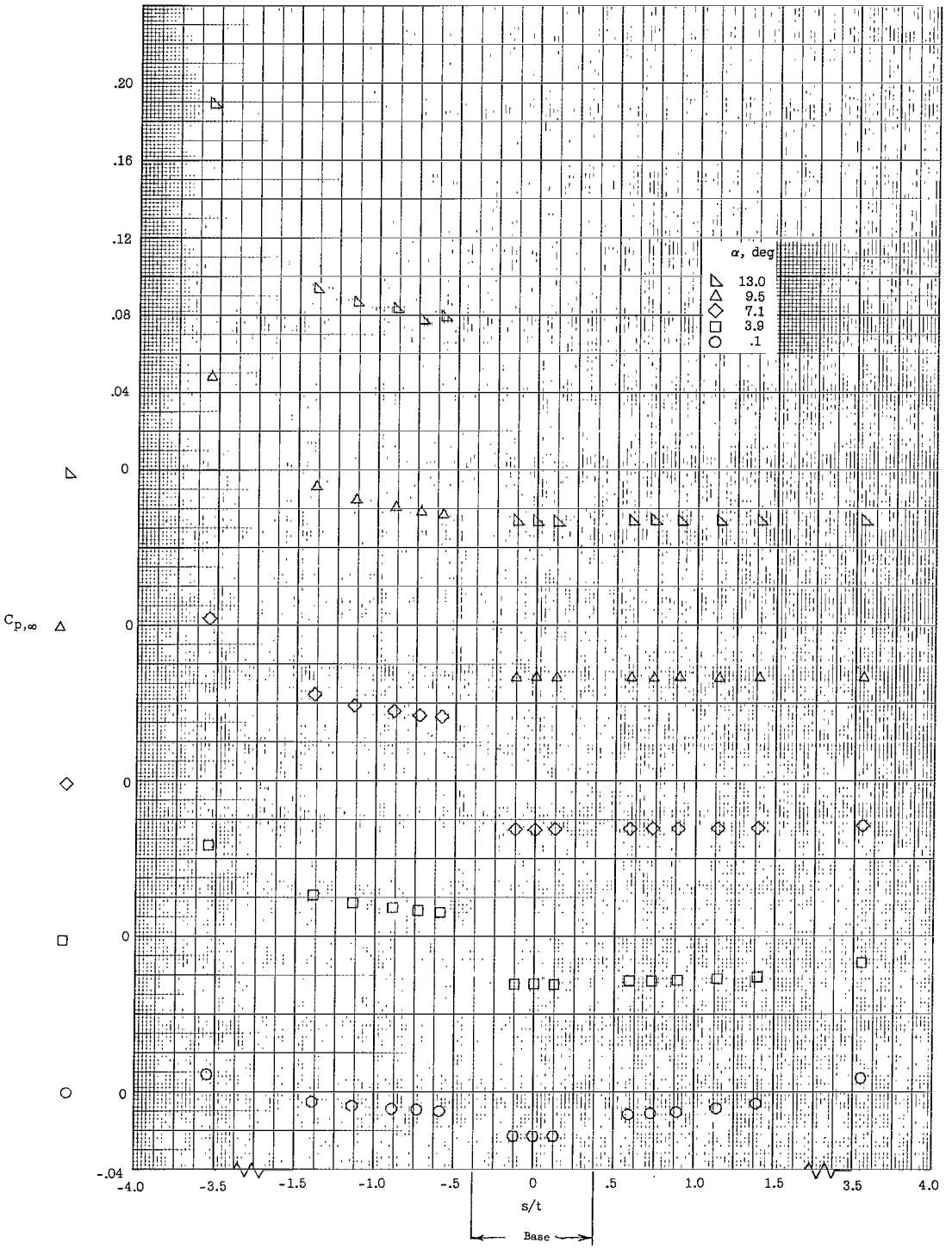

(c) $\beta = 6^{\circ}$.

Figure 4.- Continued.

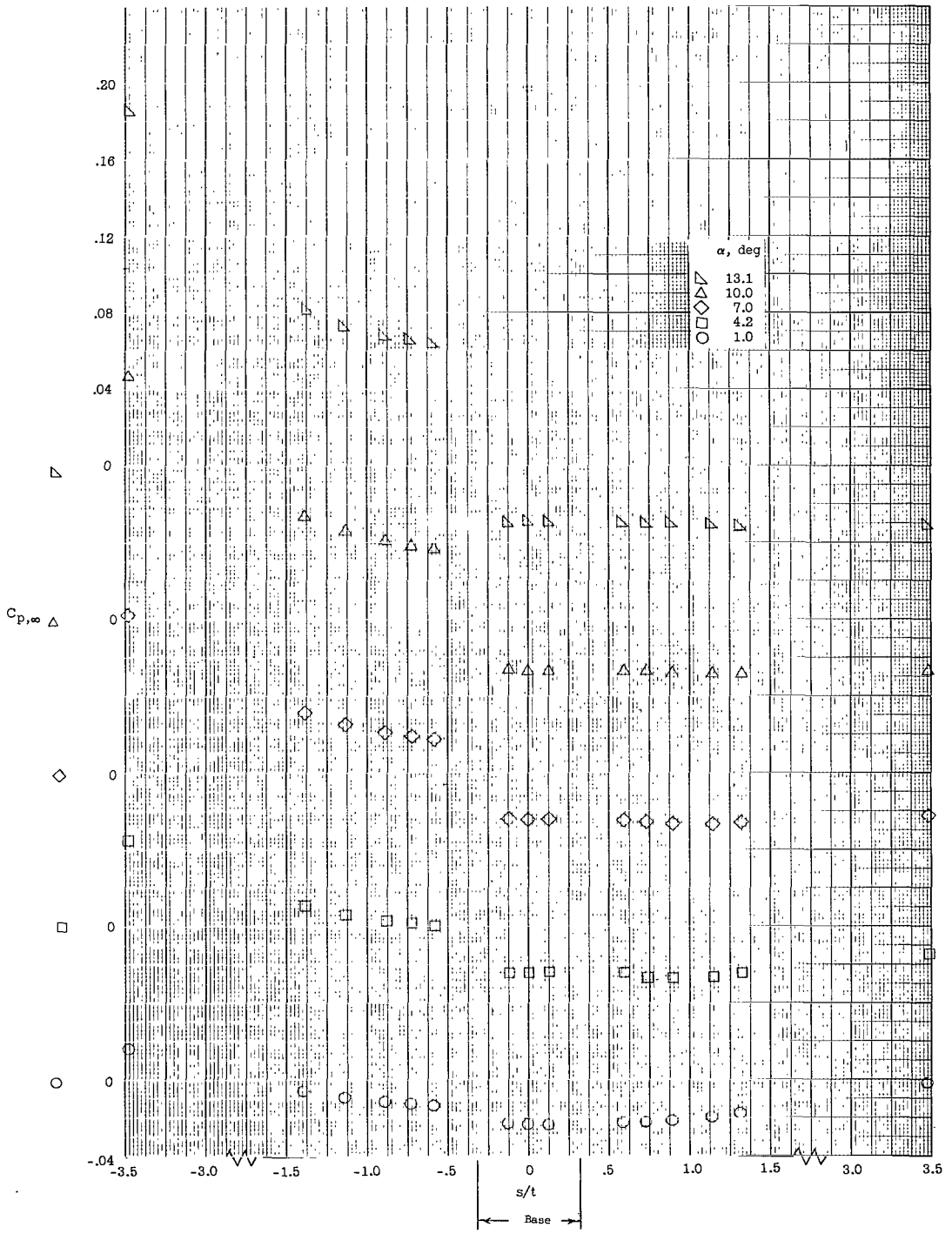

(d) $\beta = 9^{\circ}$.

Figure 4.- Continued.

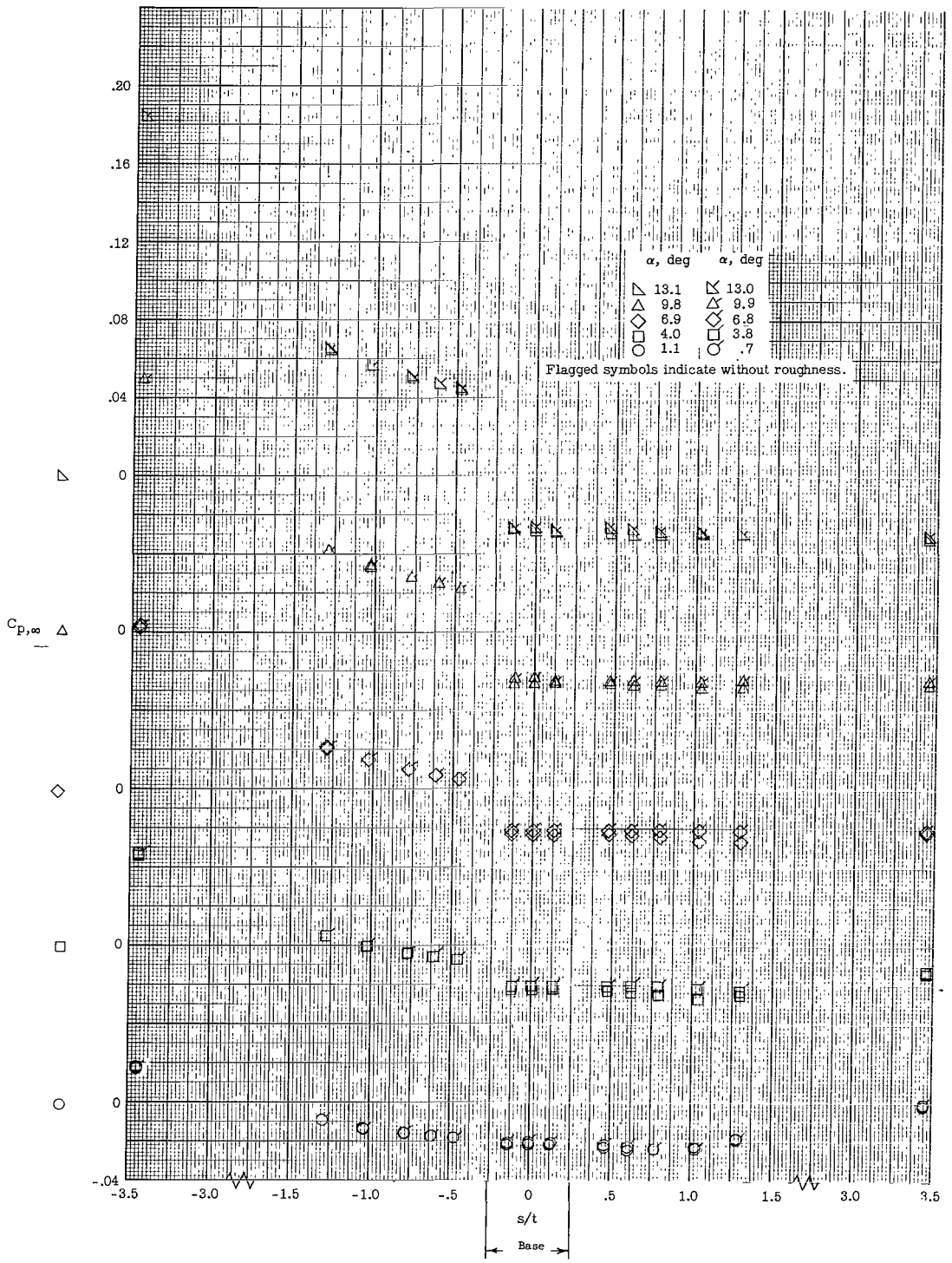

(e) $\beta = 12^{\circ}$.

Figure 4.- Continued.

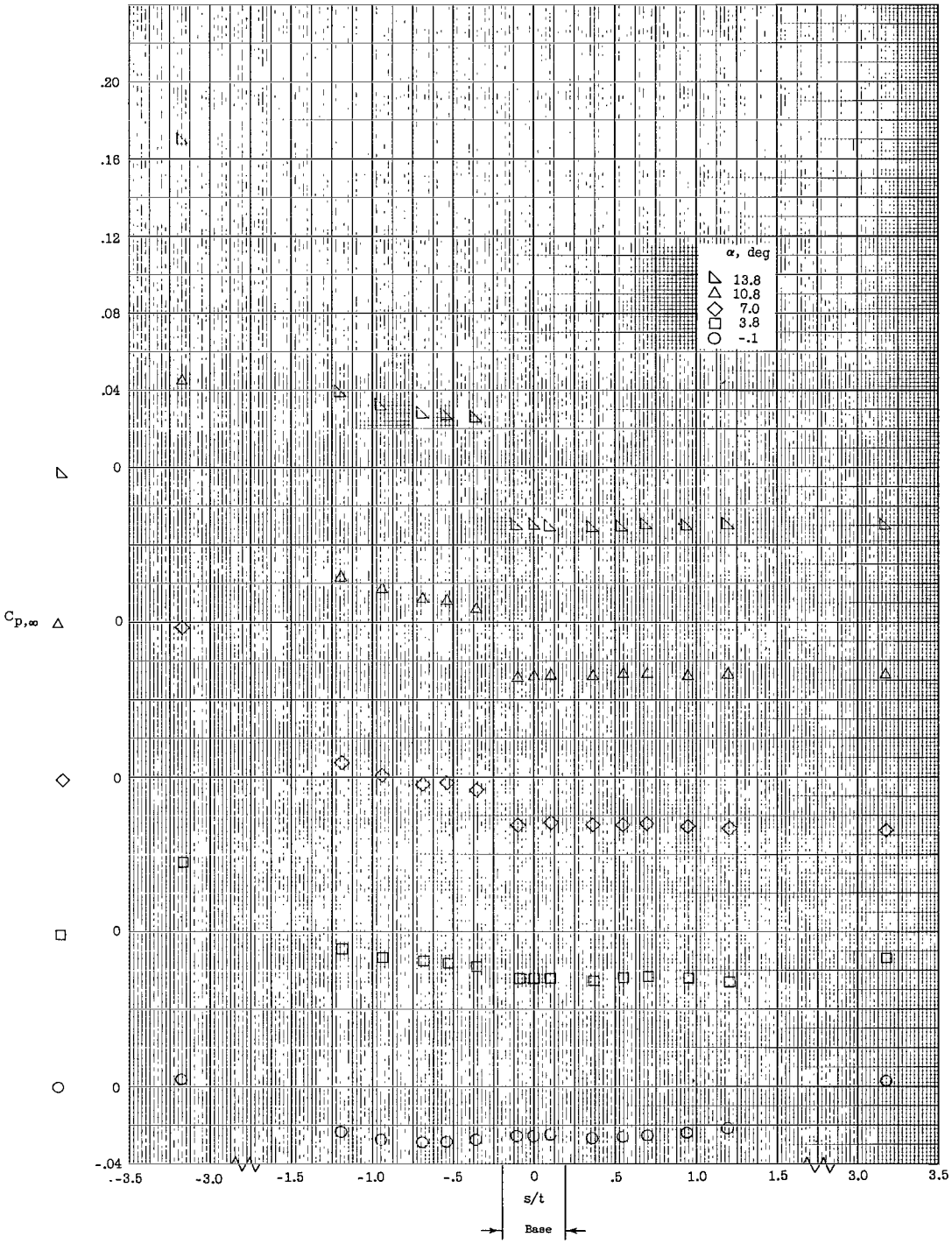

(f) $\beta = 15^{\circ}$.

Figure 4.- Continued.

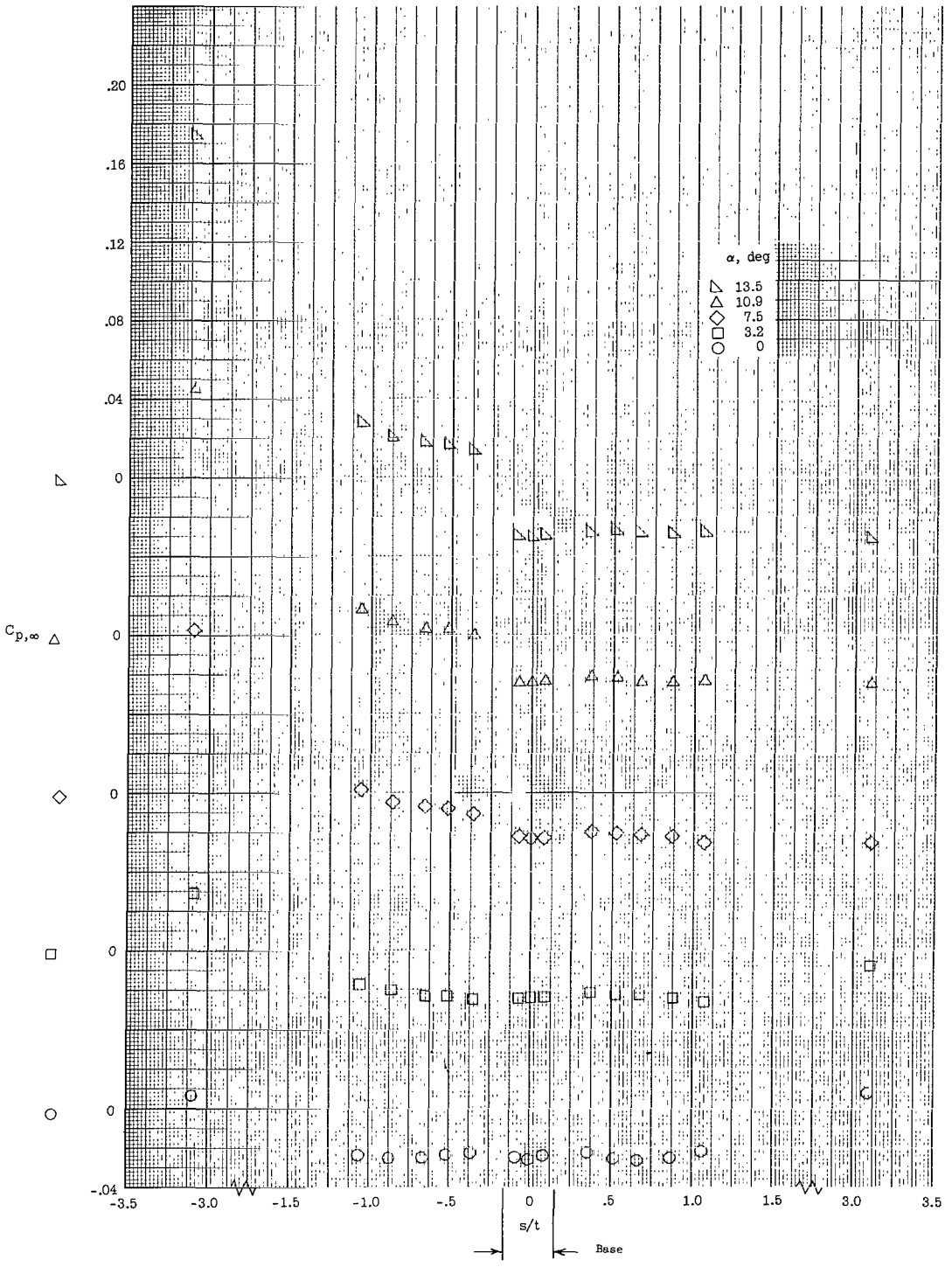

(g) $\beta = 18^{\circ}$.

Figure 4.- Continued.

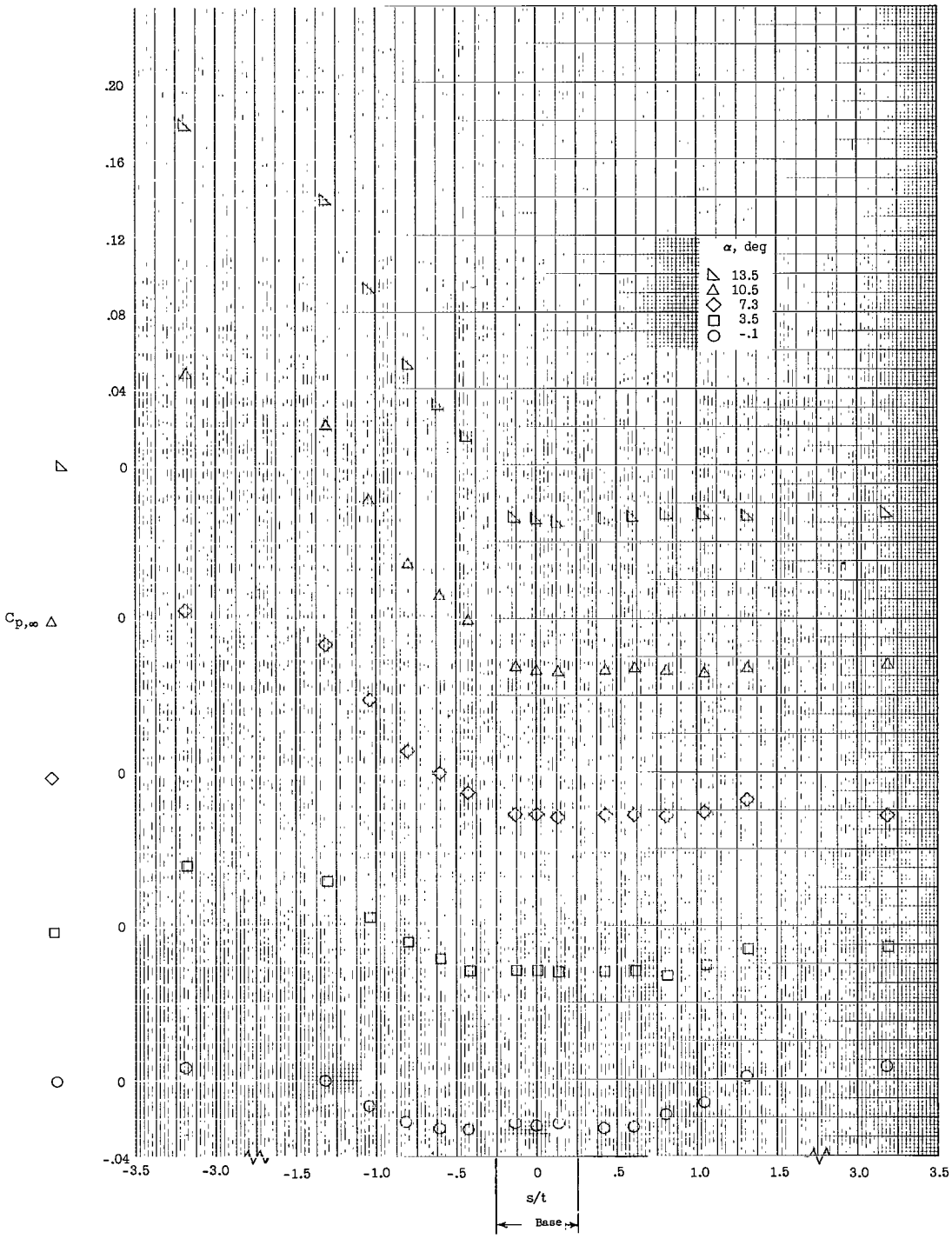

(h) Circular arc.

Figure 4.- Concluded.

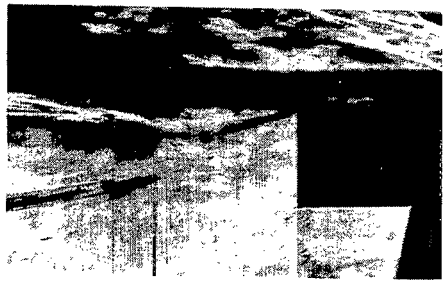

$\alpha = 0.0^{\circ}$

$\alpha = 0.1^{\circ}$

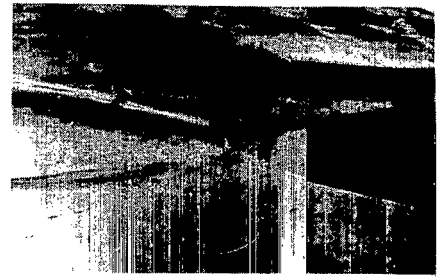

$\alpha = 1.1^{\circ}$

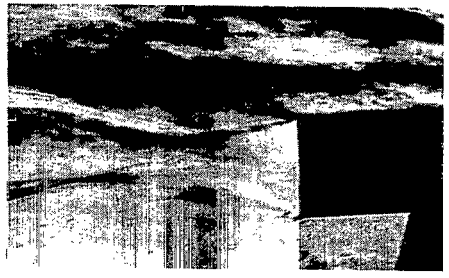

$\alpha = 3.9^{\circ}$

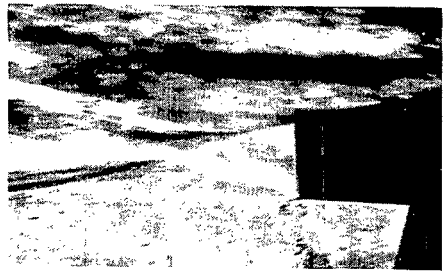

$\alpha = 3.9^{\circ}$

$\alpha = 4.0^{\circ}$

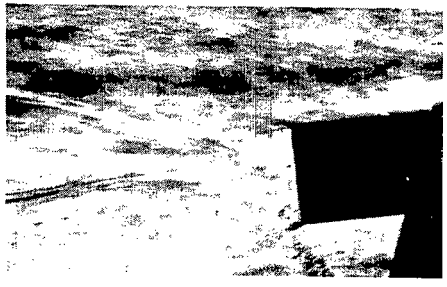

$\alpha = 6.9^{\circ}$

$\beta = 0^{\circ}$

$\alpha = 7.1^{\circ}$

$\beta = 6^{\circ}$

$\alpha = 6.9^{\circ}$

$\beta = 12^{\circ}$

Figure 5.- Schlieren photographs of flow phenomena in region of base. L-64-418

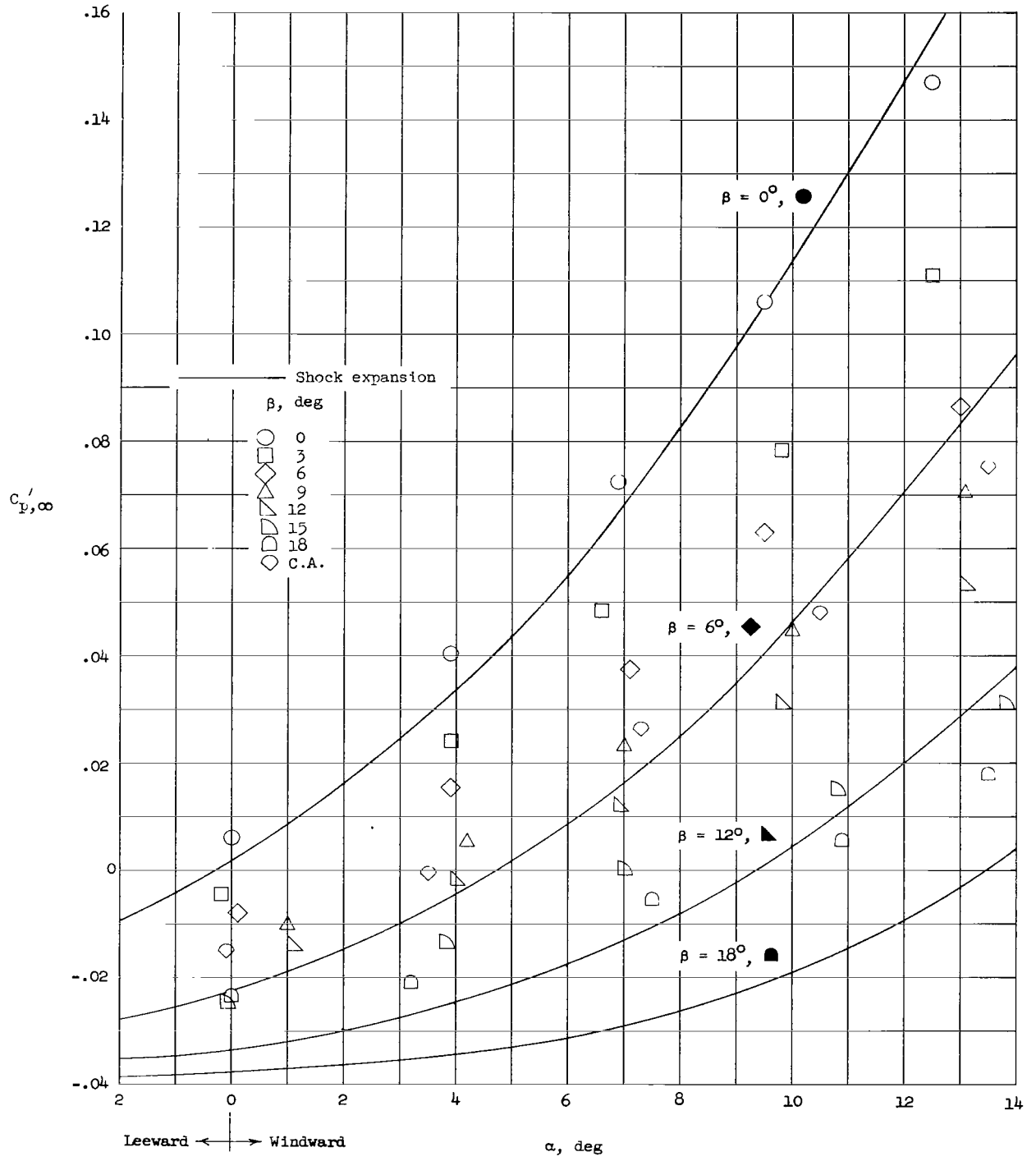

Figure 6.- Effect of boattailing on windward boattail pressures at various angles of attack.

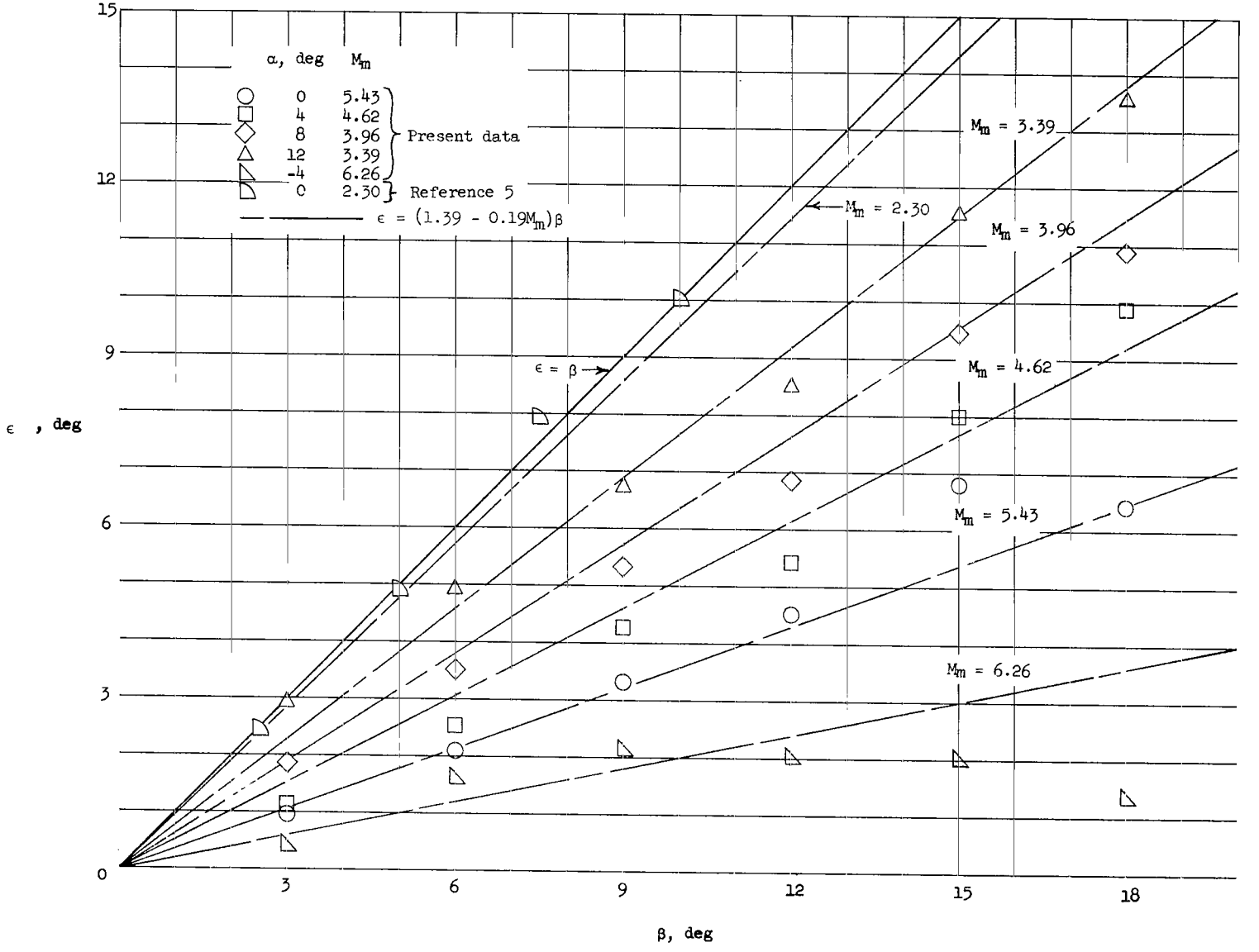

Figure 7.- Equivalent turning angle as a function of boattail angle for various surface Mach numbers.

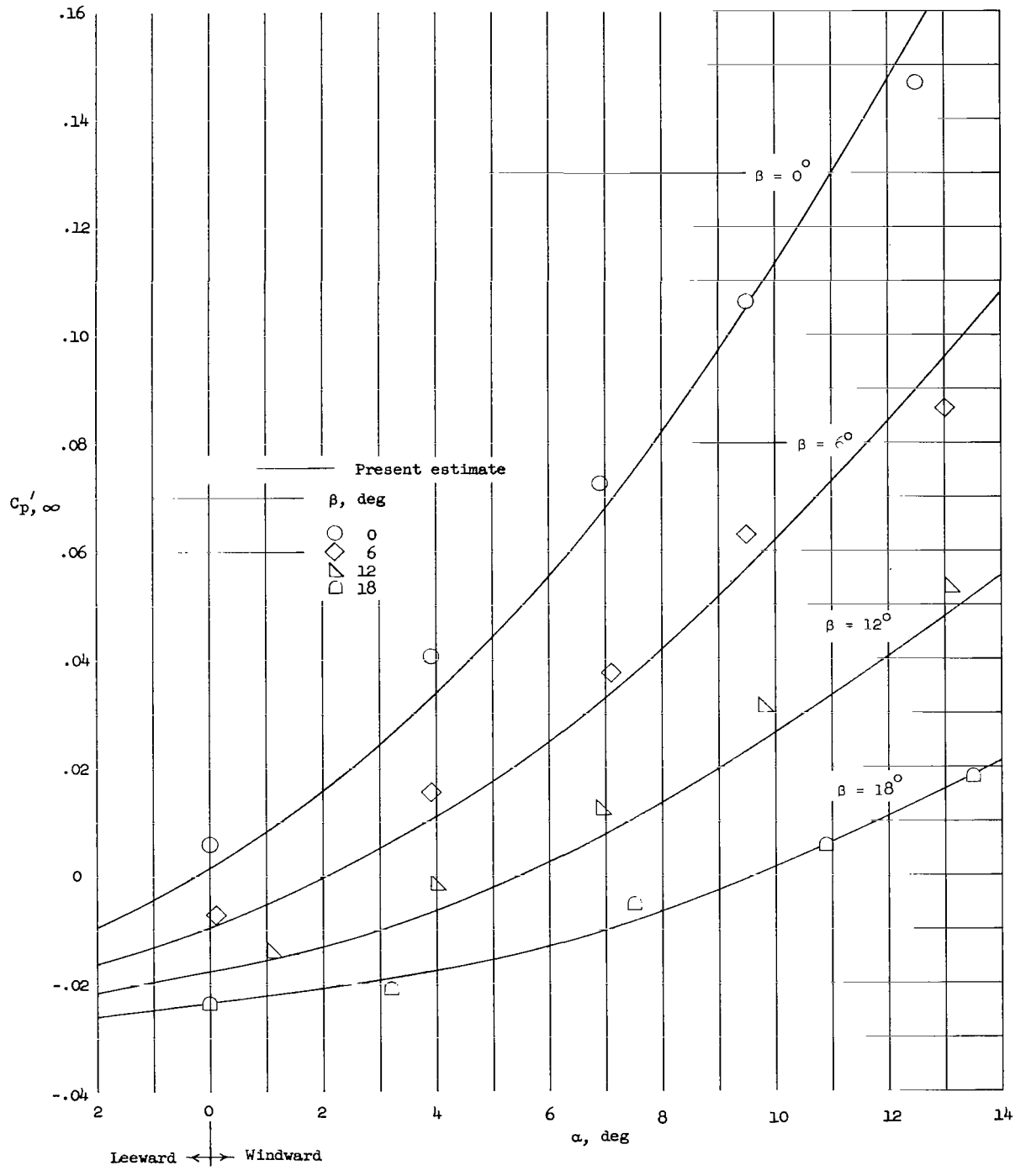

Figure 8.- Comparison of present data and estimates for windward boattails at various angles of attack.

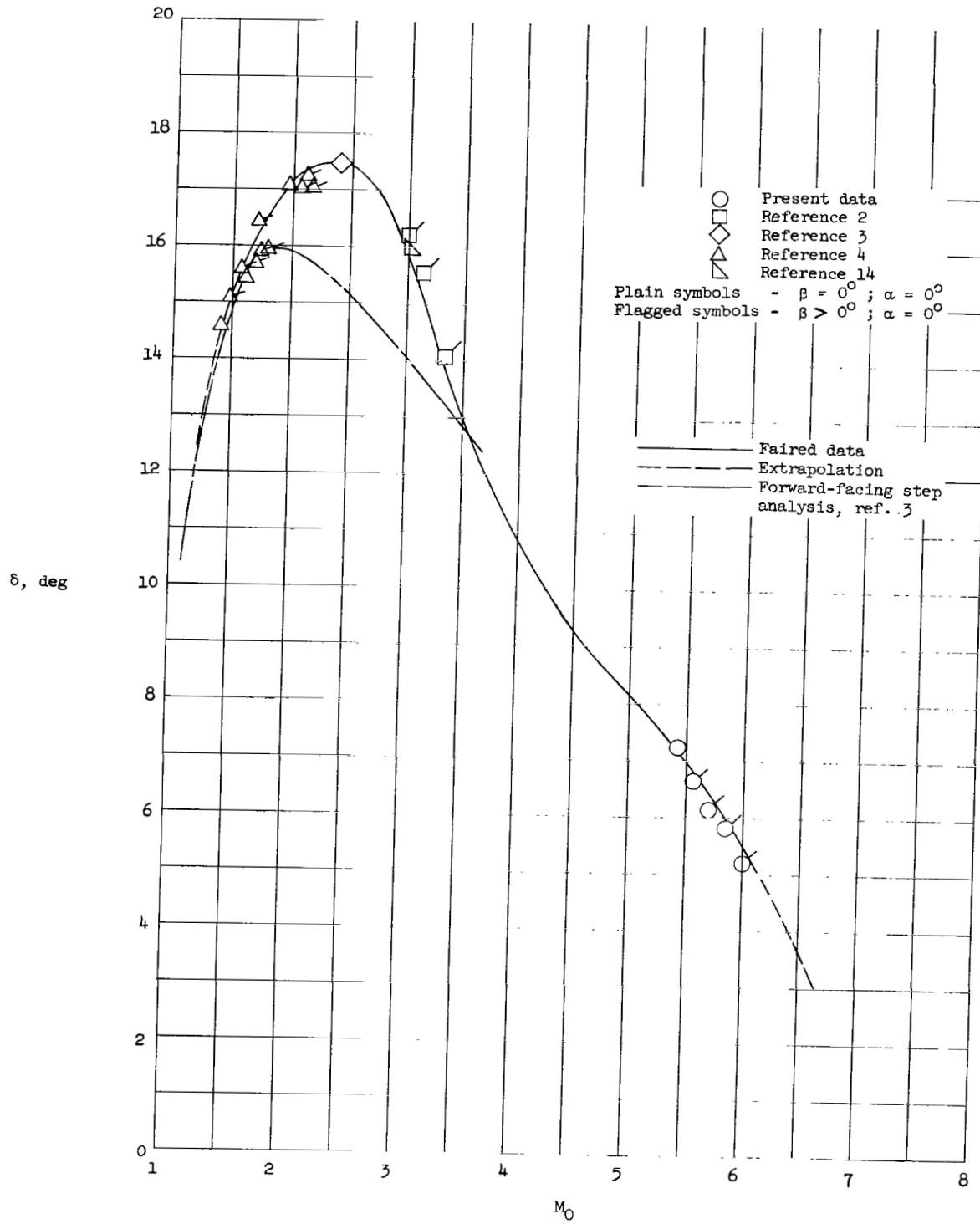

Figure 9.- Critical turning angle as a function of Mach number ahead of base.

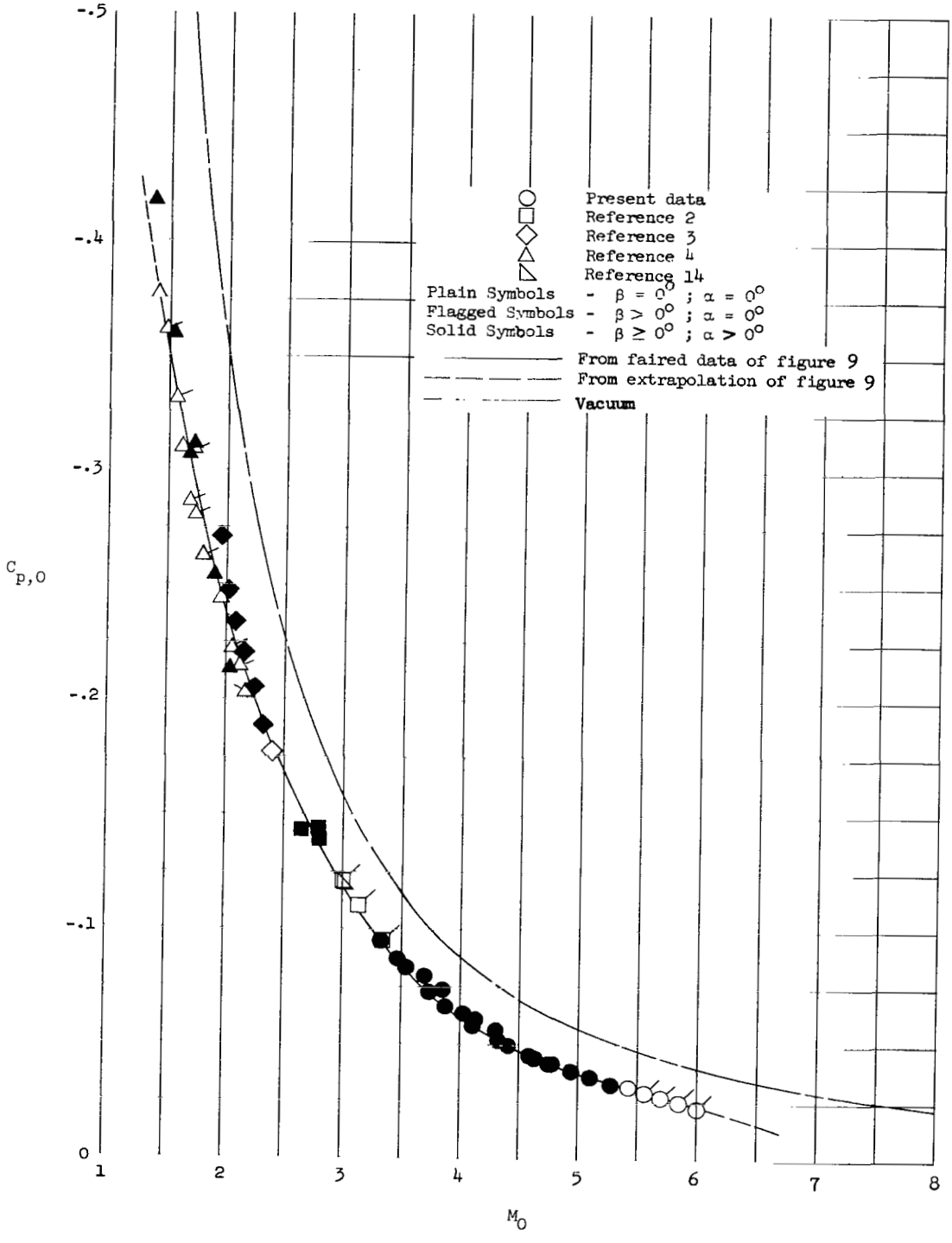

Figure 10.- Summary of base pressure as a function of Mach number ahead of base.

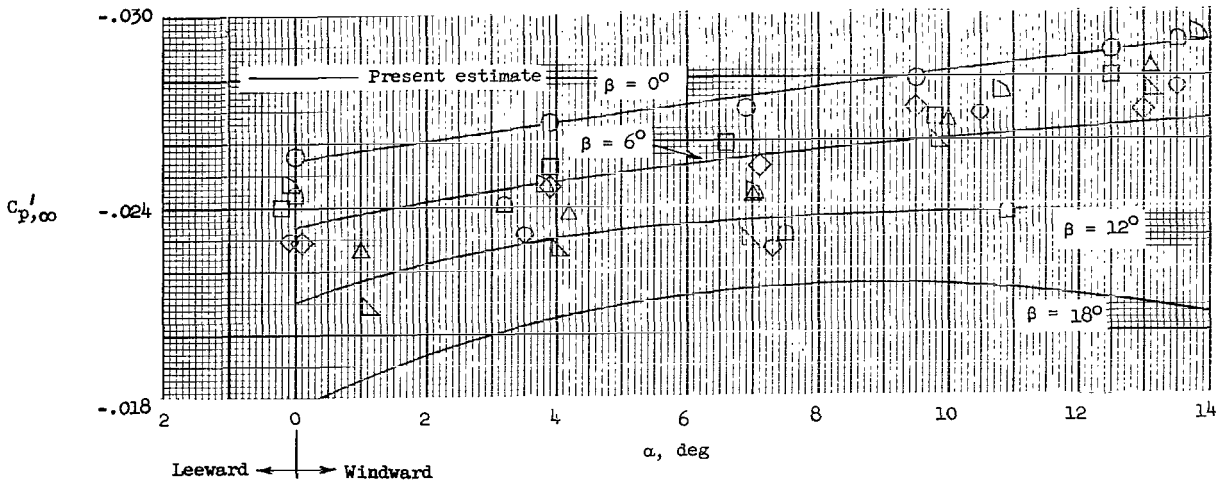

(a) Base pressures.

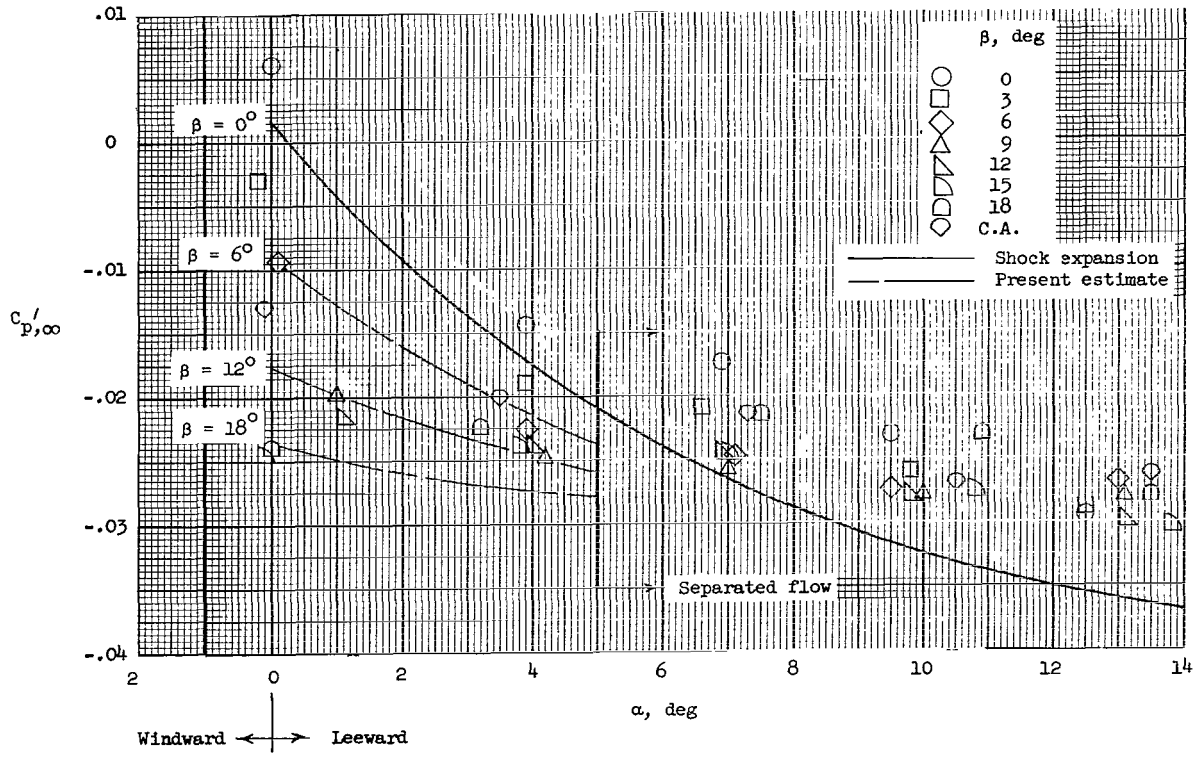

(b) Leeward boattail pressures.

Figure 11.- Effect of boattailing on base and leeward boattail pressures at various angles of attack.

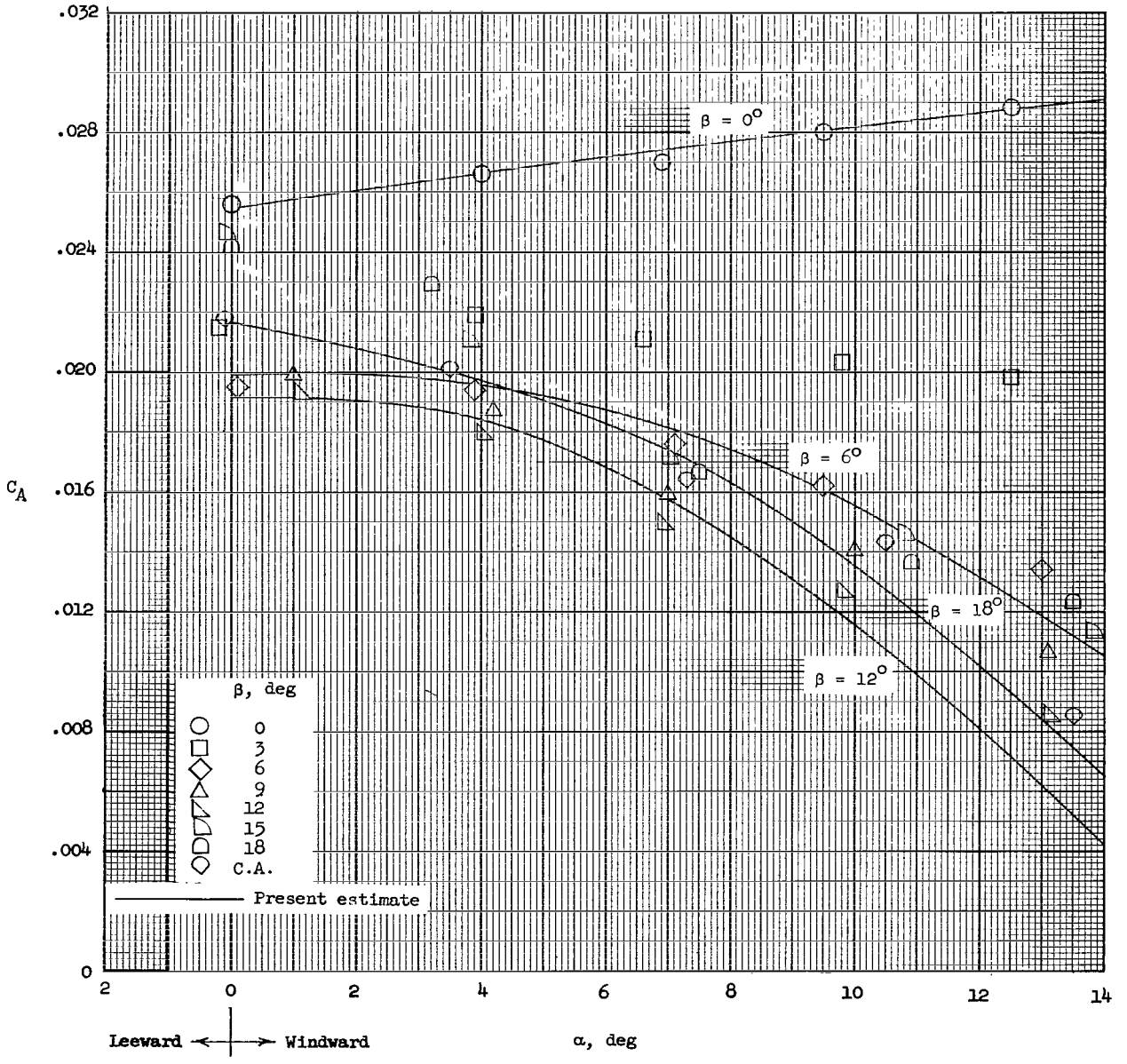

Figure 12.- Afterbody drag as a function of boattail angle and angle of attack.

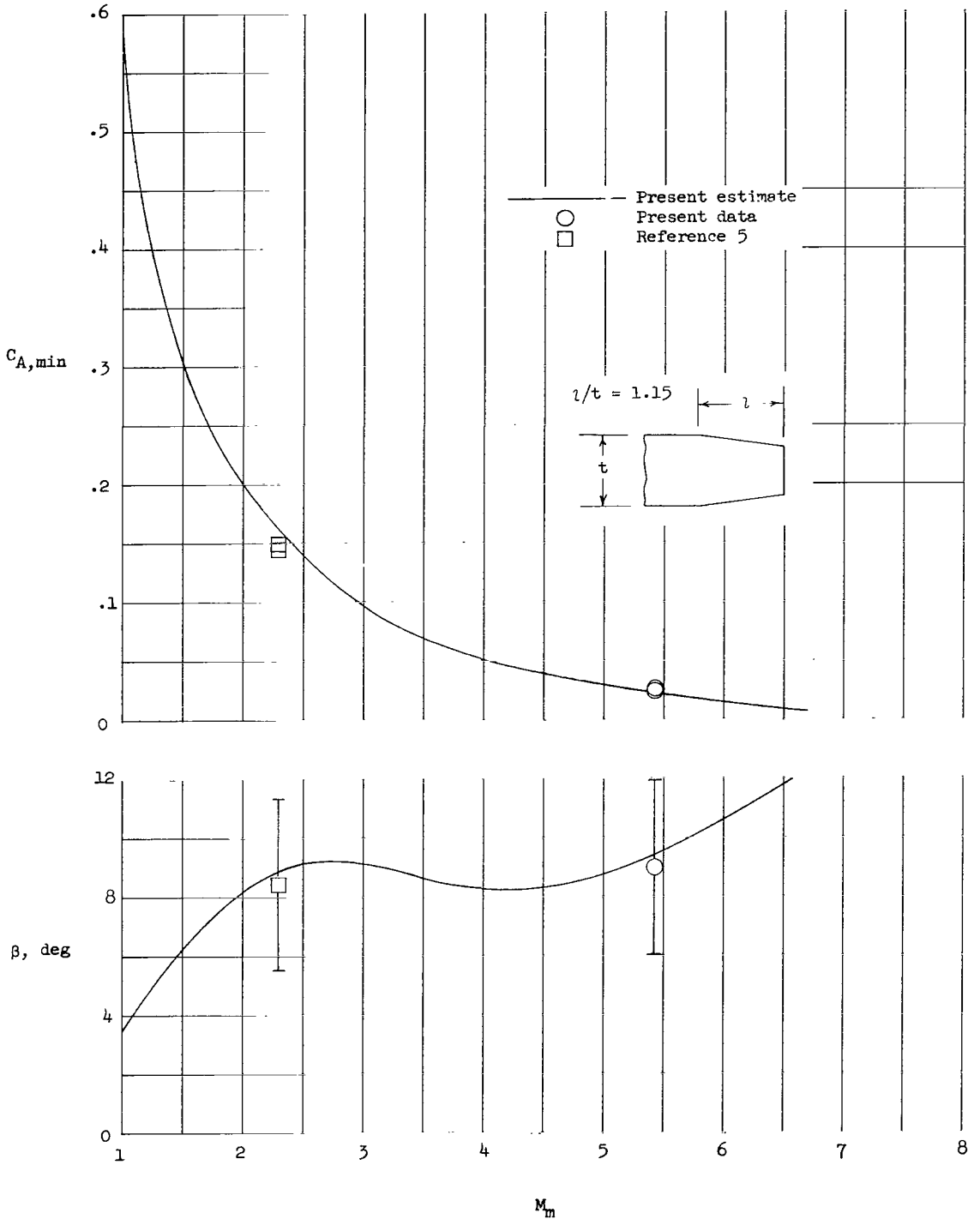

Figure 13.- Boattail angle for minimum afterbody drag at zero angle of attack as a function of Mach number ahead of base.

"The aeronautical and space activities of the United States shall be conducted so as to contribute . . . to the expansion of human knowledge of phenomena in the atmosphere and space. The Administration shall provide for the widest practicable and appropriate dissemination of information concerning its activities and the results thereof."

—NATIONAL AERONAUTICS AND SPACE ACT OF 1958

NASA SCIENTIFIC AND TECHNICAL PUBLICATIONS

TECHNICAL REPORTS: Scientific and technical information considered important, complete, and a lasting contribution to existing knowledge.

TECHNICAL NOTES: Information less broad in scope but nevertheless of importance as a contribution to existing knowledge.

TECHNICAL MEMORANDUMS: Information receiving limited distribution because of preliminary data, security classification, or other reasons.

CONTRACTOR REPORTS: Technical information generated in connection with a NASA contract or grant and released under NASA auspices.

TECHNICAL TRANSLATIONS: Information published in a foreign language considered to merit NASA distribution in English.

TECHNICAL REPRINTS: Information derived from NASA activities and initially published in the form of journal articles.

SPECIAL PUBLICATIONS: Information derived from or of value to NASA activities but not necessarily reporting the results of individual NASA-programmed scientific efforts. Publications include conference proceedings, monographs, data compilations, handbooks, sourcebooks, and special bibliographies.

Details on the availability of these publications may be obtained from:

SCIENTIFIC AND TECHNICAL INFORMATION DIVISION

NATIONAL AERONAUTICS AND SPACE ADMINISTRATION

Washington, D.C. 20546